

Effectiveness of Integration of System-Level Optimization in Concurrent Engineering for Rocket Design

by

Brian Kenichi Bairstow
B.S. Engineering and Applied Science (Aeronautics)
California Institute of Technology, 2004

SUBMITTED TO THE DEPARTMENT OF AERONAUTICS AND ASTRONAUTICS IN
PARTIAL FULFILLMENT OF THE REQUIREMENTS OF THE DEGREE OF

MASTER OF SCIENCE IN AERONAUTICS AND ASTRONAUTICS

at the

MASSACHUSETTS INSTITUTE OF TECHNOLOGY

May 2006

© 2006 Brian Bairstow. All rights reserved.

The author hereby grants to MIT permission to reproduce and to distribute publicly paper and
electronic copies of this thesis document in whole or in part, in any medium now known or
hereafter created.

Signature of Author: _____
Department of Aeronautics and Astronautics
May 25th, 2006

Certified by: _____
Olivier de Weck
Assistant Professor of Aeronautics and Astronautics & Engineering Systems
Thesis Advisor

Accepted by: _____
Professor Jaime Peraire
Professor of Aeronautics and Astronautics
Chair, Graduate Committee

Effectiveness of Integration of System-Level Optimization in Concurrent Engineering for Rocket Design

by

Brian Kenichi Bairstow

Submitted to the Department of Aeronautics and Astronautics on
May 25th, 2006 in partial fulfillment of the requirements
for the Degree of Master of Science in Aeronautics and Astronautics

Abstract

Integrated concurrent engineering is a method for rapid conceptual design. Previous study has suggested that integration of system-level optimization techniques into integrated concurrent engineering can benefit the design process. In order to confirm and strengthen these results further study was carried out.

A two-stage liquid rocket software model was created to serve as a complex multi-disciplinary design problem. Several design session trials were run with the goal of optimizing the rocket in performance and cost. Some design teams used optimization along with integrated concurrent engineering, while others only used integrated concurrent engineering. The results from the two design methods were compared in several metrics, and including optimization alongside concurrent engineering shows a marked benefit in some areas.

Thesis Supervisor: Olivier de Weck
Title: Assistant Professor of Aeronautics and Astronautics &
Engineering Systems

Acknowledgments

This work would not have been possible without many sources of help and support. I am very grateful for the time I have spent at the Massachusetts Institute of Technology. My advisor, Oli de Weck, played a huge role in giving me great advice and constructive feedback, helping me when I was stuck, and aiding me in getting my project off of the ground. I cannot imagine having done this without him. I would also like to thank my professors for the education in systems engineering and space systems that I have received. Key parts of my research would not have been possible without the facilities at MIT, in particular the Aero/Astro design lab. Fred Donovan was a big help in getting the computers up and running. Finally I'd like to thank my fellow students, both those who were great classmates, and those who were crucial to my study as participants.

Dr. Sobieszczanski-Sobieski was a big aid as well. His experience in the field was invaluable. I also appreciated Todd Schuman's help in explaining the work he had done, and getting me up to speed on the system.

My work was supported financially by the National Defense Science and Engineering Graduate Fellowship. I was honored by this opportunity from the Department of Defense.

Finally I'd like to thank my family and friends for their constant support. Having my family behind me got me to where I am today, and I hope to continue making them proud. I am very grateful for my friends, who have made college and graduate school a lot of fun. My wife Sarah has been a huge help throughout this endeavor. Her words of encouragement and technical input helped immensely, and I am lucky to have her.

Table of Contents

Table of Contents.....	7
1 Introduction.....	17
1.1 The Problem of Engineering Design.....	17
1.2 Integrated Concurrent Engineering.....	18
1.3 System-level Optimization.....	20
1.4 Combining ICE with System-level Optimization.....	26
1.5 Thesis Statement.....	28
2 ISLOCE Method.....	29
2.1 Overview.....	29
2.2 ICEMaker.....	30
2.2.1 ICEMaker Server.....	30
2.2.2 ICEMaker Client.....	31
2.2.3 ICEMaker Procedure.....	31
2.3 MOGA.....	32
2.4 Previous ISLOCE Results.....	35
3 Two-stage Liquid Rocket Model.....	39
3.1 Overview.....	39
3.2 Motivation.....	40
3.3 Rocket Dynamics.....	41
3.4 Model Overview.....	42
3.5 Model Description.....	45

3.5.1	Inputs.....	46
3.5.2	Aerodynamics	46
3.5.3	Trajectory	47
3.5.4	Propulsion	49
3.5.5	Structures	50
3.5.6	Systems	50
3.5.7	Cost	51
3.5.8	Output	52
3.6	Benchmarking.....	52
3.7	Application of the MOGA to the Model.....	53
4	Experiment Description	61
4.1	Overview.....	61
4.2	Setup	61
4.2.1	Objective	63
4.2.2	Procedure	64
4.3	Metrics	66
5	Results.....	69
5.1	Overview.....	69
5.2	Control Groups.....	69
5.3	Optimization Groups.....	74
5.4	Comparison.....	77
5.4.1	Analysis of Design Points.....	77
5.4.2	Analysis of Performance Metrics.....	80

6	Conclusions.....	89
6.1	Summary.....	89
6.2	Future Work.....	89
Appendix A	Design Session Results.....	91
A.1	Overview.....	91
A.2	Control Group 1	91
A.3	Control Group 2	92
A.4	Control Group 3	95
A.5	Control Group 4	98
A.6	Optimization Group 1	100
A.7	Optimization Group 2	103
A.8	Optimization Group 3	106

List of Figures

Figure 1-1. Design flexibility and knowledge over time	17
Figure 1-2. Example Pareto front for an airplane wing	25
Figure 2-1. Combined trade-space exploration from EFT ²	36
Figure 3-1. One-stage and two-stage rocket diagrams.....	43
Figure 3-2. Sample thrust profile	47
Figure 3-3. Sample thrust angle profile	48
Figure 3-4. Example altitude constraint functions for the 10 th and 50 th generations	55
Figure 3-5. All feasible individuals from a MOGA run	56
Figure 3-6. Non-dominated individuals.....	56
Figure 3-7. Non-dominated points from 1640 MOGA runs with constant C/m _p lines and annotations	57
Figure 3-8. Non-dominated points from 1640 MOGA runs with sample rockets plotted ¹⁵	59
Figure 4-1. Experiment procedure flowchart.....	65
Figure 5-1. Design session results from control group 2	70
Figure 5-2. Pareto fronts from all control groups	72
Figure 5-3. Design session results from optimization group 1	74
Figure 5-4. Pareto fronts from all optimization groups	76
Figure 5-5. Pareto fronts from all design sessions.....	78
Figure 5-6. Design session results and optimizer results for 1640 runs	79
Figure 5-7. Design session results and optimizer results for 2 hour MOGA computation	80
Figure A-1. Control group 1 point designs evaluated.....	92

Figure A-2. Control group 2 point designs evaluated.....	95
Figure A-3. Control group 3 point designs evaluated.....	97
Figure A-4. Control group 4 point designs evaluated.....	100
Figure A-5. Optimization group 1 point designs evaluated.....	103
Figure A-6. Optimization group 2 point designs evaluated.....	106
Figure A-7. Optimization group 3 point designs evaluated.....	109

List of Tables

Table 3-1. Master table of variables and parameters	44
Table 3-2. N ² diagram.....	46
Table 3-3. Benchmarking results	52
Table 4-1. Nominal work breakdown	62
Table 4-2. Summary of design sessions.....	63
Table 5-1. Design variables and objectives for Pareto points from control group 2	71
Table 5-2. Metric values for the control group design sessions	73
Table 5-3. Design variables and objectives for Pareto points from optimization group 1	75
Table 5-4. Metric values for the optimization group design sessions.....	77
Table 5-5. Metric values from all design sessions	81
Table 5-6. Average metric values and comparison.....	82
Table 5-7. Metric values for EFT design study ²	83
Table 5-8. Significance levels of difference in average performance metrics with one- sided t-test.....	84
Table 5-9. Average optimization group metric values and comparison to 2 hour MOGA	86
Table A-1. Control group 1 composition.....	91
Table A-2. Control group 1 feasible design points	91
Table A-3. Control group 2 composition.....	92
Table A-4. Control group 2 feasible design points	93
Table A-5. Control group 3 composition.....	95
Table A-6. Control group 3 feasible design points	95

Table A-7. Control group 4 composition.....	98
Table A-8. Control group 4 feasible design points.....	98
Table A-9. Optimization group 1 composition.....	100
Table A-10. Optimization group 1 feasible design points.....	101
Table A-11. Optimization group 2 composition.....	103
Table A-12. Optimization group 2 feasible design points.....	103
Table A-13. Optimization group 3 composition.....	106
Table A-14. Optimization group 3 feasible design points.....	106

Nomenclature

<i>BLISS</i>	= Bi-Level Integrated Systems Synthesis
<i>DDM</i>	= Design Dependency Matrix
<i>DOE</i>	= Design of Experiments
<i>DSM</i>	= Design Structure Matrix
<i>EFT</i>	= External Fuel Tank
<i>ICE</i>	= Integrated Concurrent Engineering
<i>ISLOCE</i>	= Integration of System-Level Optimization in Concurrent Engineering
<i>KKT</i>	= Karush-Kuhn-Tucker
<i>MOGA</i>	= Multiobjective Genetic Algorithm
<i>MPC</i>	= Mass Per Cost
<i>ODE</i>	= Ordinary Differential Equation

<i>A</i>	= altitude
<i>A_{target}</i>	= target orbit altitude
<i>A_{final}</i>	= ending altitude
<i>A_{stage}</i>	= staging altitude
<i>C</i>	= total cost
<i>F</i>	= fitness function
<i>g₀</i>	= gravitational constant for Earth
<i>I_{sp}</i>	= specific impulse
<i>L_c</i>	= cone length
<i>L_{f,1,2}</i>	= fuel tank length for stage 1 and 2
<i>L_{o,1,2}</i>	= oxidizer tank length for stage 1 and 2
<i>L_r</i>	= rocket length
<i>m</i>	= wet mass
<i>m₀</i>	= initial wet mass
<i>m_{engine}</i>	= engine mass
<i>m_f</i>	= fuel mass
<i>m_{final}</i>	= final wet mass
<i>m_{ox}</i>	= oxidizer mass
<i>m_p</i>	= payload mass
<i>m_{SS}</i>	= Space Shuttle engine mass
<i>m_{struct}</i>	= structures mass
<i>n_{dom}</i>	= number of times an individual is dominated
<i>p</i>	= fitness penalty from altitude
<i>q_{max}</i>	= maximum dynamic pressure
<i>r</i>	= radial position
<i>R_f</i>	= fuel tank radius
<i>R_o</i>	= oxidizer tank radius
<i>R_r</i>	= rocket radius
<i>T_{1...T₅}</i>	= thrust profile parameters
<i>T_{max}</i>	= max thrust
<i>T_{SS}</i>	= Space Shuttle max thrust
<i>t_{f,1,2}</i>	= fuel tank thickness for stage 1 and 2
<i>t_{o,1,2}</i>	= oxidizer tank thickness for stage 1 and 2
<i>t_r</i>	= rocket shell thickness
<i>v</i>	= total velocity
<i>V_{f,1,2}</i>	= fuel tank volume for stage 1 and 2
<i>V_{o,1,2}</i>	= oxidizer tank volume for stage 1 and 2
<i>α</i>	= thrust vector deviation from normal
<i>α₁, α₂</i>	= thrust angle profile parameters
<i>ΔV</i>	= change in velocity – delta V
<i>v_a</i>	= first axial mode frequency

ν_b = first bending mode frequency
 μ = standard gravitational parameter for Earth
 θ = longitude
 θ_c = cone half-angle
 ρ = atmospheric density
 ρ_{al} = aluminum density
 ρ_f = fuel density
 ρ_o = oxidizer density
 ρ_{ti} = titanium density

1 Introduction

1.1 *The Problem of Engineering Design*

Engineering design is a fundamentally difficult problem. It is necessary to simultaneously consider numerous design variables, constraints, objectives and issues, many of which are unknown at the beginning of the design process. The classic inverse design knowledge and flexibility curves hold here (Figure 1-1), as the most important decisions must be made when the designers have the least experience and knowledge, locking the design in potentially unfavorable situations even when more information is discovered. This makes preliminary design of basic form and function particularly important and troublesome.

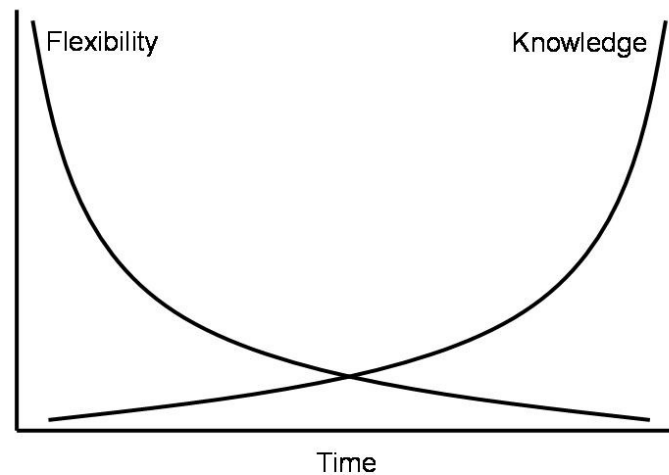


Figure 1-1. Design flexibility and knowledge over time

Multidisciplinary design is especially challenging. A common definition for a discipline is an area of work that falls under a set of governing equations. For example, aerodynamics is a discipline under the Navier-Stokes equations, and economics is a

discipline under the laws of supply and demand. Design in a single discipline is simpler because there is much less need to consider interfaces and propagation of changes across discipline boundaries. Aerospace engineering is typically very complex, as many different disciplines must be woven together into a whole to form a system. These disciplines include structures, aerodynamics, and propulsion, which are also the ‘subsystems’ of a system. A launch vehicle is an example of such a design problem, and thus a liquid rocket model was created as a representative of a complex multidisciplinary design problem.

Significant work has been done to address these difficulties in conceptual multidisciplinary design. Integrated concurrent engineering (ICE) is a process for effective and rapid design and analysis. System-level optimization is another valuable approach which can rapidly discover strong designs, or explore many designs. These tools are individually very strong and possess great potential to be used together, but are not easily combined. They are described in further detail below.

1.2 Integrated Concurrent Engineering

The traditional method of engineering design involves a number of people working separately on their areas of expertise. Communication typically happens in discrete instances like meetings, and all the work is done between meetings back at individual offices. A consequence of this arrangement is that when problems are discovered that affect other subsystems, the designers of those subsystems are not necessarily promptly notified, and work that they do can become obsolete or invalid. Furthermore, each engineer tends to focus on his own subsystem and does not fully consider the

repercussions of his work on other subsystems. An example in the context of an airplane wing would be that an aerodynamics engineer would want a high wing span to chord aspect ratio for better lift and drag performance, without realizing that this would lead to a larger mass in the structures subsystem to support the wing loading due to a larger wing root bending moment.

Often the procedure for design is to have the more constrained subsystems, or the 'drivers,' complete their designs first. Then that work is taken as a starting point for the next subsystem to be designed around. In this manner an aerodynamics engineer might try to minimize wing mass by using a large aspect ratio. The structures engineer is then forced to support that wing by using a large structural mass. It may have been the case that an intermediate wing design would have been less massive overall, if the structures engineer could have had input on the aerodynamicist's wing design. The problem could be more severe for the last subsystems in the design order, which could have to face large difficulties in squeezing their systems into remaining mass, volume, or power budgets, or have other troubles with being overconstrained due to shortsightedness from lack of communication. Furthermore, when we look beyond design to manufacturing, testing, operation, and maintainability, we see that considering these facets early in design can save a lot of time and money in the future. It is inefficient to complete a design and find out it cannot be built, or to complete production and have a system that is expensive to maintain because of the absence of an access panel that could have been added cheaply.

Concurrent engineering is a technique designed to solve these problems. The idea is to bring the subsystem engineers together to work on the system design in the same

room. Working face to face can solve many of the problems with lack of communication and understanding that come from working separately and meeting occasionally. It allows for real-time communication that can troubleshoot problems as they are discovered, and negotiate interfaces between subsystems.

Integrated concurrent engineering takes the process forward another step. Using this technique, the designers work on computers linked via a network. This allows for a high rate of information transfer as people work simultaneously on the same project. Each subsystem engineer can post their interfaces to a database on the network, which allows other people to immediately update these values and see the effects on their own subsystems. Using the design of a communication satellite as an example, the ICE process allows for rapid propagation of change when a decision such as shrinking the antenna aperture is made. In order to maintain the bandwidth, an increased power supply is needed, so the power subsystem engineer can increase the solar array surface area. The thermal subsystem engineer would need to increase the radiator size, and the structures engineer would have to confirm that the spacecraft could accommodate the new solar arrays and radiators. By linking software models and tools, this entire exchange can take place almost instantaneously.

1.3 System-level Optimization

When exploring the design space, it is necessary to quantitatively define each design that is analyzed. Typically a set of variables is used which are collectively referred to as the ‘design vector,’ or individually as ‘design variables,’ and each design vector represents a design, or ‘design point.’ If there is a tool modeling the design, then

these design variables are essentially the inputs to that model, and can be changed by the designers to form new design points. Example design variables for an airplane wing might be span and chord.

When comparing designs, it is necessary to have one or more metrics to determine which design is best. These are referred to as ‘objective variables’ or ‘objective functions,’ and are essentially the outputs of the design. Typically the goal is to minimize or maximize each of the objectives. For an airplane wing, the objective function might be to minimize the weight or maximize the lift to drag ratio.

Other outputs of a design have to do with ‘constraints,’ which are requirements on the design that must not be violated. For example, an airplane wing would have to be structurally sound and provide enough lift. These are not considered objectives because the goal is only to meet the constraints, not minimize or maximize them. With the airplane wing example, it is only necessary that the wing be sound; it is not desirable to overdesign it to a large degree. Thus in evaluating a design, certain outputs are compared to their constraint values; if the design meets every constraint it is considered ‘feasible,’ and if any constraint is violated the design is ‘infeasible.’ Constraints can be inequalities or equalities.

The combination of a design vector, an objective function, and constraints defines an optimization problem. The design vector is adjusted to maximize or minimize the objective function. This is conceptually simplest for a single objective, as in theory one could explore all combinations of design variables and use the extrema found as the

results. This would be a full-factorial search of the design space, but there are several more sophisticated methods.

One class of algorithms for numerical optimization is referred to as gradient methods. This method takes a starting point and incrementally moves in the direction that improves the objective function the most. Each step involves choosing a step direction and step size, starting from an initial point. In a situation with two design variables and one objective variable, the objective could be plotted over the design variables as a contour map. Assuming the goal is to maximize the objective, a basic gradient algorithm would go from the starting point up the path of steepest ascent until it reached the top of a hill for maximization or bottom of a valley for minimization. At that point the Karush-Kuhn-Tucker (KKT) optimality conditions would be met. This is also true if the optimal point is not an interior point, but one where one or more constraints are active. If the underlying objective function is convex then the KKT conditions are both necessary and sufficient for a global optimum. A risk with using a gradient algorithm is that it is possible to get stuck with a result other than the global optimum if the space is non-convex, which means that one can have local extrema. This outcome can be ameliorated by running the optimization from multiple starting points, but this increases the computation time without definitely solving the problem.

Another approach to optimization is to use one of many heuristic methods. A heuristic method applies a simple rule of thumb, often derived from natural processes, combined with some amount of stochasticity to an optimization problem. Most heuristic methods incorporate randomness, which effectively allows the optimization to escape

local extrema. While not guaranteed to find the global optimum, they can perform relatively well in complex, non-convex problems with both continuous and discrete design variables; problems with which numerical (gradient) optimizers have difficulty.

One heuristic technique is the genetic algorithm. Genetic algorithms are inspired by natural selection, a biological process in which the ‘fittest’ individuals tend to survive, thereby optimizing the population. Thus, rather than optimizing a single point design like a gradient optimizer, a genetic algorithm works with a population of individual design points. Each individual is defined by its design vector, which also acts as the individual’s ‘chromosomes.’ The individual is evaluated via a fitness function, often identical to the objective function. At each step, or generation, individuals are selected from the population according to their fitness functions, and the individuals then ‘mate’ in random pairs to produce the next generation. The children produced by mating can have a random combination of the parents’ genes, and additionally there is a chance of mutation for additional randomness and facilitation of change. This continues until the population arrives at a configuration that meets a threshold of stability, for example going ten generations without a change to the fittest individual. If the population keeps changing, the algorithm will typically end when some specified number of generation is reached.

When multiple objectives are introduced, it is rarely the case where all objectives are optimized at the same point, so there is no clear single optimal point design. A multiple-objective problem can be reduced to a single-objective problem by simply taking a weighted average of the objectives. The problem here is that it is difficult to choose an appropriate weighting, since without expert knowledge of the situation any

weighting would be arbitrary. Additionally it has been shown that optimizing weighted sums with sweeping weights from one extreme to another can lead to poorly distributed solutions in objective space and can right out miss points in non-convex areas of the objective space. A solution to this problem is, in a sense, to consider all possible weightings. Essentially if a design is ‘dominated’ (another feasible design exists that performs better in every objective) then it cannot be the optimum for any weighting. If a design is ‘non-dominated’ (no feasible design exists that performs unilaterally better than it) then a weighting exists that would make that point the optimum, unless that point is in a concave region of the objective space. This means that the result of the optimization is not a single point and is instead a set of points. These points would be the family of non-dominated designs, which is called the ‘Pareto front,’ even though in many cases we can only find approximations to the true Pareto front. Since every point on the Pareto front is non-dominated, when you move from one point to another you are trading one objective for another, effectively shifting the weightings of the objective. The airplane wing example could be made into a multi-objective problem by introducing cost as a second objective to be minimized, as shown in Figure 1-2. The ‘utopia point’ is the point that takes the best values for each objective, in this case in the lower left corner with both the minimum cost and minimum mass found. While being mathematically defined, the utopia point is not physically realizable due to design variable bounds, constraints and the domain of the underlying objective functions.

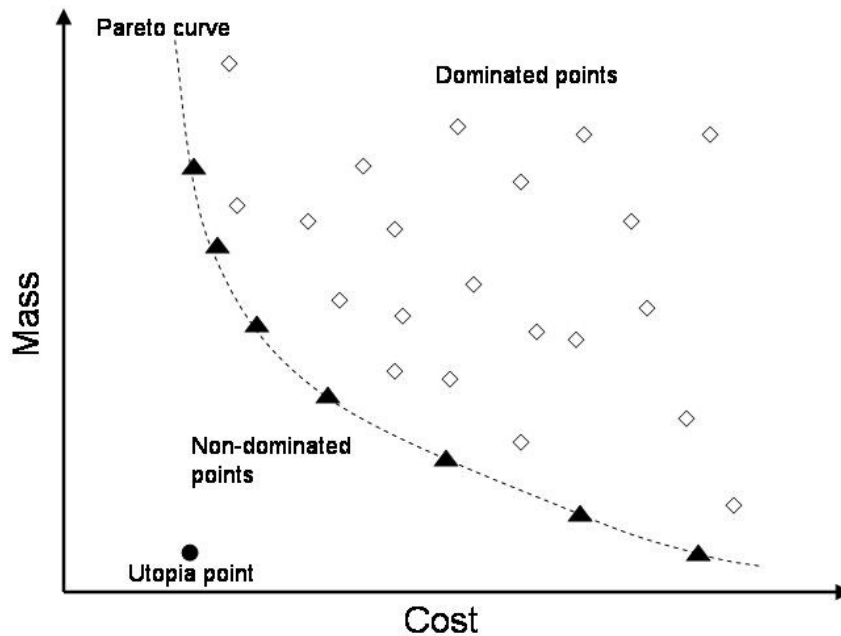


Figure 1-2. Example Pareto front for an airplane wing

Genetic algorithms adapt well to a multiple-objective optimization problem. Since they already use a family of point designs at each step, they naturally explore the design space to help find a Pareto front. Choosing a fitness function becomes more difficult for a multi-objective genetic algorithm (MOGA), since it is no longer possible to simply use the objective function without using weighting. One general way to solve this problem is to have fitness based on domination: individuals that are non-dominated have full fitness, while those that are dominated have less fitness depending on how many individuals dominate them. This avoids requiring arbitrary weightings, and also promotes populating the Pareto front, since the members considered most fit are non-dominated. This is valuable because the Pareto front is the desired output of the optimization, since it can give the designer a range of possible non-dominated designs to investigate.

1.4 Combining ICE with System-level Optimization

Both ICE and system-level optimization are strong techniques, but there are difficulties in combining the two. Subsystem-level optimizers are already commonly used in ICE, since subsystem engineers use them as tools in design. This is significantly different from system-level optimization, since subsystem-level optimization can be done without considering interfaces to other subsystems. The advantage of system-level optimization is that it seeks the overall best result, and does not optimize one subsystem to the detriment of others. The difficulties are the added complexity, and thus the time to both formulate and run the optimization. Since the ICE process strives to produce accurate results very quickly, it would not find much use in an optimization that takes weeks to write or run, as might be expected of an optimizer for a real-world system of high complexity. Advances in computing, and usage of lower-fidelity optimization help reduce the runtime. A low-fidelity model can be optimized in real-time and thus used in ICE design sessions. The system-level optimizer can be used to quickly survey the design space and find promising design points using lower fidelity models that can then be explored by the design team using appropriate high fidelity models, which would be of benefit to the ICE process. Some methods, like Bi-Level Integrated Systems Synthesis (BLISS), have been proposed and tested to accomplish this in an automated fashion.¹ In BLISS 2000, subsystems publish maps of input-output relationships using lookup tables, response surfaces or other surrogate models, while a system optimizer mines these models using various weightings for subsystem objectives to achieve an overall system-level optimization. This thesis takes a similar approach but focuses specifically on how system optimization and ICE, with humans-in-the-loop, may be combined.

Clearly, optimization benefits from being combined with ICE; while optimization is a powerful computational tool for finding effective designs, the results of the optimization are not useful without trade studies and human analysis. Post-optimization analysis gives information about the design space and the performance of the optimizer. Furthermore, the results of the optimization are only as good as the person who creates the optimization process, whose knowledge would have to be comprehensive of all the subsystems and therefore not as specialized as the subsystem experts. Thus, if combined effectively, it is expected that ICE and optimization can benefit greatly from each other.

Work by Schuman explored the advantages of including optimization in the design process by comparing concurrent design of the Space Shuttle external fuel tank (EFT) with and without optimization as a tool.² He had two groups work in an ICE session on the EFT design, and included optimization in the process for one of the two groups. The results showed a slight improvement when including optimization, but with only one test point it was difficult to prove a statistical increase in design efficiency. In order to achieve more definitive results, a larger sample size must be used. Further, it is expected that a more complex design problem – beyond the limits of a single humans' cognitive limit – will increase the gap in effectiveness between the optimization and control groups. This is because increasing the number of inputs can make the problem more difficult to grasp, in accordance with the concept that the human mind performs well up to the range of “ 7 ± 2 ” variables.³

1.5 Thesis Statement

The objective of this thesis is to test the hypothesis that a multi-objective genetic algorithm used in parallel with integrated concurrent engineering allows for more complete exploration of the Pareto front of design points of a rocket model during a rapid conceptual design process than integrated concurrent engineering alone. This study demonstrates any benefits of using system-level optimization to augment integrated concurrent engineering. To compare design with and without optimization, live trials were used in which teams were tasked with exploring the design space and populating the Pareto front.

2 ISLOCE Method

2.1 Overview

Schuman developed the framework of Integration of System-Level Optimization in Concurrent Engineering (ISLOCE).² The ISLOCE method combines the strengths of ICE and system-level optimization to promote rapid conceptual design. The two processes work in parallel: in the foreground team members work on the problem using the ICE method, while the optimizer operates in the background. The optimizer periodically provides outputs which can be leveraged by the design team.

Schuman's ISLOCE process also includes the use of neural networks to parameterize the design team subsystem models for faster implementation and optimization. Neural networks are decomposable mathematical models that are well suited for learning a task. The parameterization addresses the problem that optimization is a slow process and allows it to be run in real-time. The neural networks act as approximations of the subsystem models, and the optimizer links these lower-fidelity models together to quickly find interesting designs for the team to investigate. The neural network technique is important to making ISLOCE a viable method for real problems, but was not utilized for this study. This is because the optimization was able to be implemented ahead of time, the computational load was not too high, and the focus of the study was the change in design performance gained by using system-level optimization in ICE, rather on showing it to be possible.

For this study, the ICE process was implemented using ICEMaker, and the optimizer was a multiobjective genetic algorithm (MOGA). These tools are described below in greater detail.

2.2 ICEMaker

ICEMaker is software for facilitating the ICE process, and was created at the California Institute of Technology Laboratory for Spacecraft and Mission Design.⁴ ICEMaker allows for parameter transfer and data storage during a design session, using an Excel and Visual Basic implementation. The ICEMaker framework consists of a central server and a number of client modules. The client models break the problem down, often into the subsystem level, and are coded into Excel spreadsheets. The interactions between the clients are passed through the server as parameters, using Visual Basic macros. As an example of a parameter interaction for a satellite modeled in ICEMaker, the communications subsystem might have “communications power required” as an output, and the power subsystem would have that as an input in order to size the power generation and energy storage.

2.2.1 ICEMaker Server

At the center of ICEMaker is the database where all of the parameters are stored. This database receives the outputs from and provides the inputs to the client sheets when these actions are requested. The server also tracks errors such as multiple subsystems trying to output the same parameter. For this reason, a consistent naming convention is very important, to make sure parameters are not duplicated. Finally the server stores all

the parameters at the end of the session, so those parameters can be loaded back up to look at the results.

2.2.2 ICEMaker Client

The ICEMaker client Excel workbooks are user-created models which are coded offline with the level of fidelity desired. They are typically both created and run by the same person, who is referred to as the subsystem chair. There are a few special spreadsheets in a client module. The inputs sheet has a list of parameter names that the subsystem uses as inputs, and a list of the corresponding values of those parameters. The values are not updated continuously from the database, but instead only when requested by hitting the “Request” button which is tied to a macro. This keeps the values from being overwritten when the client chair does not expect it. The outputs sheet has a list of the parameters that the subsystem outputs to the server, and the values of those parameters which are linked in from calculations throughout the model. The project status sheet has a list of all parameters available from the subsystems, as well as a list of parameters that people are requesting that are not currently provided by any client. This allows for visualization of the interfaces between the subsystems, helps catch errors in the parameter naming, and promotes discussion about the work breakdown between the subsystems. Finally, there can be any number of calculations spreadsheets according to the user’s preference, and these are where all of the subsystem modeling takes place.

2.2.3 ICEMaker Procedure

Once subsystem models have been created as client spreadsheets, the first step in an ICEMaker session is to load up the server on a central network location, and have each

subsystem chair open up their client spreadsheets. This is best done in a computer lab with sufficient workstations. To commence the session, each chair sends the outputs from his client to populate the server parameters and test that everything is working. There should be some discussion of the session goals, and the design variables should be set. At this point the clients should begin to request inputs from the server, perform internal calculations, and send the output results back to the server. This process usually needs to be done in a certain order to make sure calculations are done with the right data, according to the way information flows between the subsystems. A N^2 -diagram (Design Structure Matrix (DSM) or Design Dependency Matrix (DDM)) can be helpful in understanding the flow of information and any iterations that may be required. For example, for a satellite model, the power subsystem might be better placed at the end of the sequence so that the information about power requirements from each subsystem is available to size the power system. There are often feedback loops in which the subsystems depend on each other cyclically, and these make it necessary to run through the subsystems several times to iterate to a converged solution. Once a solution is found, then the team should discuss the results, discuss the next point design or trade study to examine, and begin the procedure again with a new input vector.

2.3 MOGA

The multi-objective genetic algorithm is a powerful tool to produce a family of non-dominated designs, performs well in complex design spaces, and handles discrete variables.⁵ These are all reasons why a MOGA is suitable for exploration of a complicated system. The particular implementation used for this study was adapted from work by Schuman.² Several settings are important to the functioning of this MOGA.

The design variables must be selected and given lower and upper bounds so there is a finite design space. As the design vector is encoded into bits, the number of bits must be specified for each design variable. For a continuous variable, a large number of bits would be necessary for high fidelity, while for a discrete variable, just having a few bits could cover all the cases. The user must also choose the number of individuals per generation, and the number of generations to run before ending. Increasing the number of individuals can give a more diverse population, and increasing the number of generations can give the algorithm more time to settle to an optimum. However, the product of these two numbers will usually be the number of necessary design evaluations, and is therefore directly proportional to the computation time. The crossover and mutation rates are other parameters which can be set. The crossover rate is the chance that pairs of individuals selected to advance are combined and ‘mated.’ The alternative is that the individuals move on the next generation unchanged. The mutation rate is the chance that individual bits in the individual will be changed randomly. Mutation allows the population to escape from local optima, but setting the rate too high makes it difficult for the population to converge.

The fitness function is central to the MOGA, as it is the mechanism used to select which individuals survive and which are discarded. For a multi-objective problem it is no longer obvious that the fitness function should be the same as one of the objective functions. It is possible to weight the multiple objectives and form a fitness function, but this is somewhat arbitrary. To promote finding a family of optimal designs, it is useful to define the fitness as a measure of non-domination. One scheme is to start each individual at an initial, maximum fitness. Then a small penalty is assigned for each other individual

that dominates that individual by performing equally or better in every objective (and better in at least one objective). Further penalties are assigned for constraint violations. A penalty that increases as the violations worsen will promote the optimizer to find feasible results. Overall, this fitness method means that the Pareto-front points are the most fit, which is consistent with the desire to optimize a family of designs.

The design vectors must be assigned for the initial population, which is the set of individuals for the first generation of the algorithm. The initial population could be seeded with designs from earlier studies, or could be random, where each individual has each design variable assigned randomly between the lower and upper bounds.

After the optimization is initialized, it can begin processing the generations. At each generation, each individual is evaluated to find the performance characteristics, and the fitness of each individual is measured according to the fitness function. Then members are selected for the next generation. The members are selected randomly and proportionally by fitness value for this study. Individuals are paired up and perform crossover with a chance given by the crossover rate. Mutations then occur according to the mutation rate. At this point the next generation population is finalized, and the procedure begins again.

After the maximum number of generations is reached, the result from the full MOGA run of generations is a large number of design points. The designs that violate constraints can be screened out, leaving only the feasible individuals. At this point dominance filtering can be carried out to find the non-dominated points and form a Pareto front.

Since the MOGA is a heuristic method, there is built-in randomness. In this case the randomness comes from the initial population, and the member selection, pairing, crossover chance, and mutation chance at each generation. Thus the results from separate runs can be very different in design and performance. Running the MOGA multiple times can give broader variety to the families of points, and give a greater understanding of the design space by superposition of results obtained from separate MOGA runs.

2.4 Previous ISLOCE Results

Schuman performed interesting initial work on the ISLOCE including live trials on the Space Shuttle external fuel tank design.² The objectives were to maximize payload mass and to minimize cost, in order to produce a tank capable of holding the most fuel while remaining affordable. The results from this study will be briefly discussed here.

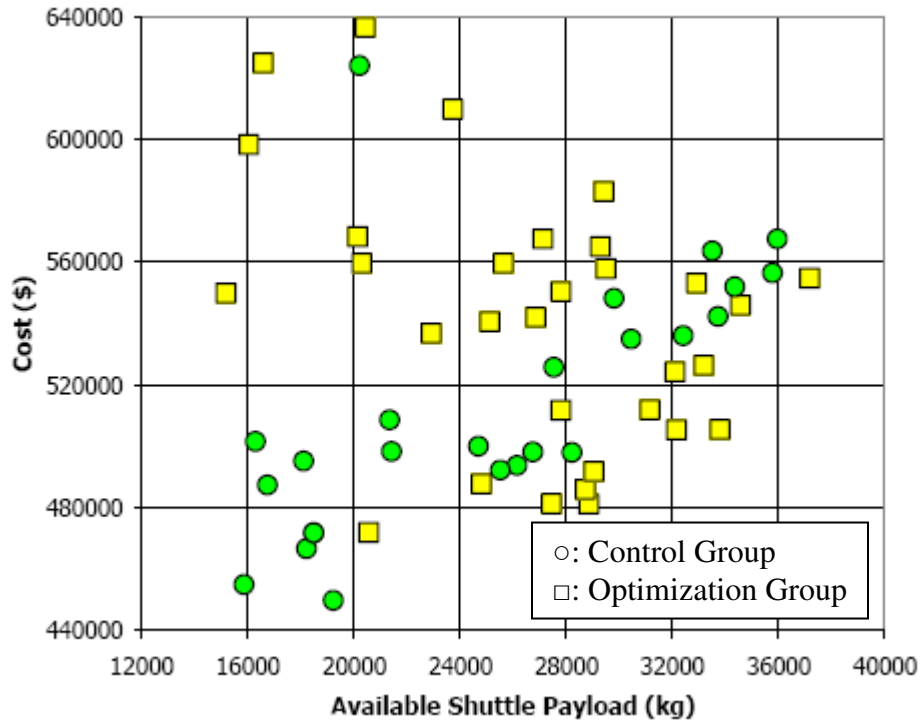


Figure 2-1. Combined trade-space exploration from EFT²

In Figure 2-1 we see some of the final results from Schuman’s work.² The design points from the control and optimization groups are plotted together, and several observations can be drawn. The optimization group has a large number of points that are clearly dominated, but the points that are non-dominated are closer to the utopia point than the best control group points. The control group explored a wider range of points, and found more points in the low-cost region. Another contribution from this work was the formulation of metrics to make more quantifiable and meaningful comparisons between the control group and the optimization group. These metrics are described in section 4.3.

The results from the previous study suggest advantages and disadvantages for the optimization method, but it is difficult to prove the statistical significance of the results.

The results could have been affected by chance or capabilities of different members on the two teams, and a larger sample size could address these issues.

3 Two-stage Liquid Rocket Model

3.1 Overview

In order to investigate the advantages of optimization in the design process, it was necessary to have a context for comparison. Having a software model for a design problem which allows for analysis of a design point then allows for quantitative design studies and optimization. By using a problem with moderate complexity and ten to twenty design variables and some amount of internal coupling, it was expected that optimization would provide sufficient advantage to show a statistically significant improvement.

With these characteristics in mind, the model created for the ISLOCE study was a two-stage liquid rocket model.⁶ The model has fifteen design variables in different disciplines which define the rocket structure, geometry, and trajectory. There are several interactions between the rocket subsystems and nonlinearity and a non-convex design space, which leads to a fairly difficult design problem.

The motivation for optimization of a rocket model is described in the next section. The basics of rocket theory and the description of the rocket model follow. The results of the benchmarking the model are discussed, as well as results of system-level optimization of the model.

3.2 Motivation

The purpose of a launch vehicle is the safe transfer of a payload from the surface of the Earth to orbit. In this case the target orbit has been defined as a circular Low-Earth Orbit (LEO) at an altitude of 400 km, but this can be adjusted based on mission needs.

It is advantageous to increase the payload mass a rocket is capable of transporting while keeping other characteristics constant. A larger payload capability enables new mission concepts such as larger space telescopes or more capable Mars rovers. It also has the potential to reduce cost, because a mass surplus allows for use of less expensive materials and simplifies the engineering task. A rocket manufacturer also has incentive to improve payload capability, since doing so could potentially increase demand and therefore profits.

Another valuable change would be to decrease the rocket cost while keeping performance constant. Cheaper rockets can lower program costs, making it easier for NASA programs to gain congressional approval and avoid cancellation. Lower launch costs can enable commercial space ventures such as communication satellites and space tourism. From the outlook of a rocket manufacturer, a lower cost to build a rocket will increase the profit margin, or allow for a lower sale price and increase demand.

It follows that one method for rocket optimization is to increase payload mass and decrease cost at the same time. This is formally stated in Eq. (3.1) and Eq. (3.2).

$$\text{Maximize } J_1 = \text{Payload Mass (metric tons)} \quad (3.1)$$

$$\text{Minimize } J_2 = \text{Cost (\$)} \quad (3.2)$$

System-level rocket optimization studies typically use a constant payload mass, and the objective function is to minimize the rocket gross mass.^{7,8,9} The model used for this study instead uses initial wet mass as an input and optimizes by maximizing payload mass. This different approach leads to a survey of the design space rather than a specific design, and this type of design is well-suited for testing of the ISLOCE method.

3.3 Rocket Dynamics

The purpose of a rocket is to propel a payload. From the equations of motion, we know that acceleration is equal to force divided by mass as in Eq. (3.3), and for constant mass this can be integrated to get Eq. (3.4) and Eq. (3.5).

$$a = F/m \quad (3.3)$$

$$v = v_0 + t \cdot F/m \quad (3.4)$$

$$x = x_0 + v_0 t + t^2 \cdot F/(2m) \quad (3.5)$$

However, since a rocket carries its own fuel, the mass changes over time. This complicates the situation, and leads to the rocket equation shown in Eq. (3.6).

$$\Delta V = g_0 I_{sp} \ln(m_0/m_{\text{final}}) \quad (3.6)$$

Here ΔV is the change in velocity, g_0 is the acceleration due to gravity on Earth, I_{sp} is the specific impulse of the rocket engine, and m_0 and m_{final} are respectively the initial and final masses of the rocket.

The rocket equation applies well to in-space transfers, but for rocket launches from planetary surfaces there are additional complications. The rocket equation assumes that the only force acting on the rocket is the engine thrust, but for rocket launches there are non-negligible gravity and drag terms. The rocket equation can still be used by approximating these contributions as a flat ΔV penalty based off of empirical data, or a more rigorous method can be used.

The shooting method is a technique which can be used to solve the equations relating to rocket launch. In this method, an ordinary differential equation (ODE) is numerically solved in order to incorporate the gravity and drag terms. One possible state vector is [radial position, radial velocity, angular position, angular velocity, mass]. The radial acceleration would be a function of the gravity term, centripetal acceleration, and the thrust and drag in the radial direction. The angular acceleration would be a function of the thrust and drag in the radial direction. The mass rate of change would be a function of thrust.

3.4 Model Overview

The model was built largely from first principles, and started as a single-stage liquid rocket. Previous work at the Massachusetts Institute of Technology was used as a starting point, which influenced the structures and propulsion design significantly.¹⁰ The cost model was adapted from a simplified Space Shuttle external fuel tank cost model.¹¹ The model was initially coded in MATLAB.

The basic model structure of the single stage liquid rocket is depicted in the left side of Figure 3-1. The rocket has a cylindrical body and is capped with a cone. The rocket dimensions are determined by the radius R_r and the length of the propellant tanks. The propellant tanks hold the oxidizer and fuel, and are cylinders capped with hemispheres. The denser oxidizer is placed on top because this allows a greater control torque from gimbaling the engine, though that effect is not modeled in the current system.

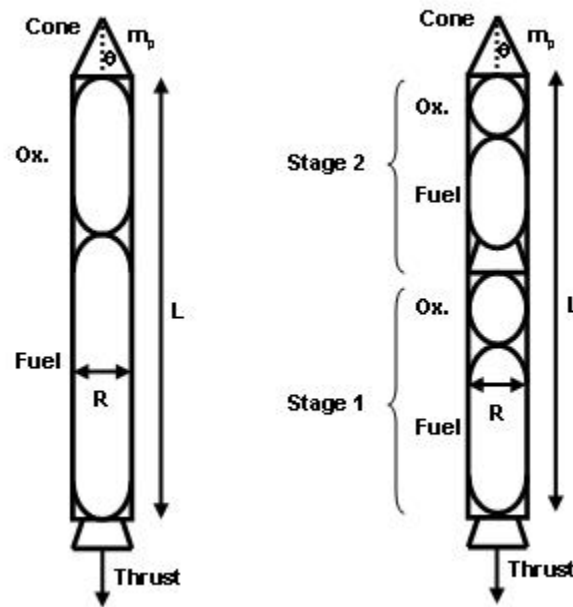


Figure 3-1. One-stage and two-stage rocket diagrams

The single-stage model was expanded into a two-stage model (depicted in the right half of Figure 3-1) by treating the second stage as the payload of the first stage and applying the single-stage model twice. At a certain altitude, the rocket drops the first stage tanks and engine, and the model uses the ending conditions of the first stage as the initial conditions for the second stage. These conditions include velocity, position, and mass.

As stated previously, there are two objective outputs from the model: payload mass and cost. The payload mass should be maximized and the cost minimized. There are three more outputs that act as constraints, the ending altitude and the frequencies of the first axial and bending modes of vibration. There are fifteen inputs to the system which define the design vector. These design variables are the initial wet mass, the rocket radius, the cone half-angle, five parameters describing the thrust profile, two parameters describing the thrust-angle profile, the altitude at which to stage, the propellant types to use in stage one and stage two, and the structural materials used in the rocket body and tanks. The objectives, constraints, and design variables are included in the master table in Table 3-1. The master table also includes a list of dependent variables that are used internally in the model, and a list of parameters which remain constant.

Table 3-1. Master table of variables and parameters

Name	Symbol	Unit	Description
Objectives			
payload mass	m_p	[kg]	objective
cost	C	[\$]	objective
Constraint Outputs			
ending altitude	A_{final}	[km]	constraint
axial mode freq.	v_a	[Hz]	constraint
bending mode freq.	v_b	[Hz]	constraint
Design Vector			
initial wet mass	m_0	[kg]	design variable
rocket radius	R_r	[m]	design variable
cone half-angle	θ_c	[rad]	design variable
thrust profile	$T_1 \dots T_5$	[N]	design variable
angle profile	ca_1, ca_2	-	design variable
staging altitude	A_{stage}	[km]	design variable
fuel type – stage 1		-	design variable
fuel type – stage 2		-	design variable
structure material		-	design variable
tank material		-	design variable
Rocket Dimensions			
length	L_r	[m]	dependent
thickness	t_r	[m]	dependent
cone height	L_c	[m]	dependent

Name	Symbol	Unit	Description
Oxidizer Tank Dimensions			
radius	R_o	[m]	dependent
length	$L_{o,1,2}$	[m]	dependent
thickness	$t_{o,1,2}$	[m]	dependent
oxidizer volume	$V_{o,1,2}$	[m ³]	dependent
Fuel Tank Dimensions			
radius	R_f	[m]	dependent
length	$L_{f,1,2}$	[m]	dependent
thickness	$t_{f,1,2}$	[m]	dependent
fuel volume	$V_{f,1,2}$	[m ³]	dependent
Parameters			
air density	ρ	[kg/m ³]	parameter
oxidizer density	ρ_o	[kg/m ³]	parameter
fuel density	ρ_f	[kg/m ³]	parameter
aluminum density	ρ_{al}	[kg/m ³]	parameter
titanium density	ρ_{ti}	[kg/m ³]	parameter
orbit altitude	A_{target}	[km]	parameter
initial inclination	θ_0	[rad]	parameter
final inclination	θ_f	[rad]	parameter

3.5 Model Description

The model is divided into several subsystems, and the flow of design variables is displayed as a design dependency matrix, commonly called an ‘N² diagram,’ in Table 3-2. The subsystems are in the boxes along the diagonal of the matrix. Outputs from each subsystem are shown to the left and right of the subsystem, and inputs to a subsystem are in the cells above and below. The subsystems have been ordered to have as few parameters as possible in the lower-left half, because this means that most of the parameters flow forward in a logical order of evaluation.

Table 3-2. N² diagram

Inputs	θ_c R_r	m_{wet} , T , α , R_r , A_{stage} , prop. type	prop. type	R_r , material type	m_{wet}	R_r , prop. type, material type	
	Aero	C_D		L_c , C_D		L_c	
		Traj	m_{prop} , T_{max}	v_{max} , q_{max}	A_{final} , ending conditions		A_{final}
			Prop	m_f , m_o , m_{eng}	m_f , m_o		
				Struct	m_{struct} , v_a , v_b	geometry, masses	v_a , v_b
		$m_{payload}$, 1 st stage conditions			System		$m_{payload}$
						Cost	\$
							Output

3.5.1 Inputs

The design vector comes from an external source, which could be an optimizer or a design team in the ICE process. A MATLAB script reads in the inputs and distributes them to the necessary subsystems in the order shown in Table 3-2.

3.5.2 Aerodynamics

The aerodynamics subsystem calculates the cone length via geometry, and calculates an estimate of the coefficient of drag using the simple pressure drag equation shown in Eq. (3.7). This estimate, from Newton's model for cone drag, is only used for preliminary calculations; a more complicated model is used later to account for the effects of Mach number.

$$C_D = 2 \cdot \sin(\theta_c)^2 \quad (3.7)$$

3.5.3 Trajectory

The trajectory subsystem takes in several inputs and calculates the fuel usage and final altitude via the shooting method. The thrust and thrust angle are calculated from the altitude using parameters from the design vector.

The thrust parameters T_1 , T_2 , T_3 , T_4 , and T_5 define the thrust at 0 km, 50 km, 100 km, 200 km, and 400 km altitudes, respectively. In between these altitudes the thrust is interpolated linearly. However, this approach could be adapted to use a spline instead of a simple linear interpolation. Initially the model used an exponentially decaying thrust, but this did not capture all of the characteristics of typical actual thrust profiles.^{12,13} A sample thrust profile from the model follows in Figure 3-2.

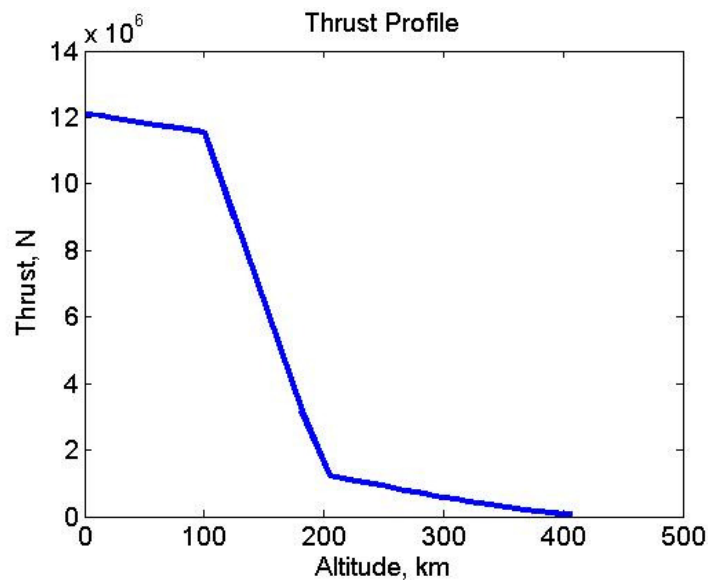


Figure 3-2. Sample thrust profile

The thrust angle parameter variables α_1 and α_2 define the angle (with respect to a normal from the Earth's surface) of the thrust vector over the course of the trajectory. α_1

is the altitude in km to start turning the rocket, while α_2 specifies the additional altitude over which to complete the turn. If the altitude is less than α_1 then the angle is zero, and if it is greater than $\alpha_1 + \alpha_2$ then the angle is $\pi/2$. If it is in between then it is defined by Eq. (3.8).

$$\alpha = [1 - \cos(\pi \cdot (A - \alpha_1) / \alpha_2)] \cdot \pi / 4 \quad (3.8)$$

A picture of the thrust angle profile for $\alpha_1 = 100$ km and $\alpha_2 = 200$ km is shown in Figure 3-3.

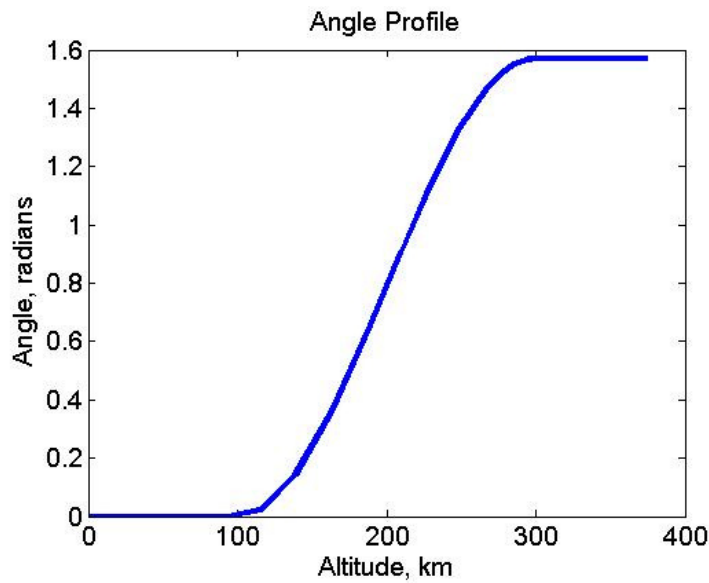


Figure 3-3. Sample thrust angle profile

To carry out the shooting method, an ordinary differential equation (shown in Eqs. (3.9-3.13)) is used with a state vector composed of radial position (r), radial velocity (r'), longitude (θ), angular velocity (θ'), and mass (m). The model calculates the changes in velocity as a function of thrust, gravity, and drag, and thrust angle. Changes in mass are calculated as decreasing according to thrust level and I_{sp} . The air density and temperature numbers are estimated using the 1962 US Standard Atmosphere model.¹⁴

$$d/dt [r] = r' \quad (3.9)$$

$$d/dt [r'] = -10^9 \cdot \mu / r^2 + r \cdot \theta'^2 + (T[r, T_1 \dots T_5] - D[r, v, \theta_c, R_r]) \cdot \cos(\alpha[r, \alpha_1 \dots \alpha_5]) / m \quad (3.10)$$

$$d/dt [\theta] = \theta' \quad (3.11)$$

$$d/dt [\theta'] = (T[r, T_1 \dots T_5] - D[r, v, \theta_c, R_r]) \cdot \sin(\alpha[r, \alpha_1 \dots \alpha_5]) / (r \cdot m) \quad (3.12)$$

$$d/dt [m] = -T[r, T_1 \dots T_5] / (I_{sp} \cdot g_0) \quad (3.13)$$

The ending condition for the ODE is either when the rocket levels off ($r' = 0$), or when the staging altitude is reached ($r = A_{\text{stage}}$). If the rocket has only carried out the first stage calculations, then the ending conditions of the ODE are output by the trajectory subsystem to be used as the initial conditions of the second stage. If the rocket has stopped gaining altitude, then the final altitude has been reached and there is an additional burn to circularize the rocket orbit. This burn is calculated using the rocket equation, where the ΔV is that necessary to adjust the velocity to that required for a circular orbit at that altitude, as shown in Eq. (3.14).

$$\Delta V = |v - (\mu / A_{\text{final}})^{1/2}| \quad (3.14)$$

3.5.4 Propulsion

The propulsion subsystem inputs the mass of propellant from the trajectory subsystem, and divides up this mass into oxidizer and fuel according to the mixture ratio for the propellant type chosen. A five percent ullage penalty is added to the propellant mass to account for the propellant that remains in the tank and lines after the burn. The propulsion subsystem also calculates the mass of the engine by scaling the Space Shuttle engine with max thrust according to Eq. (3.15).¹⁰ Differences in engine nozzle

efficiencies at different altitudes were not taken into account, which is equivalent to assuming the nozzle is reconfigurable to give full efficiency.

$$m_{\text{engine}} = T_{\text{max}} \cdot m_{\text{SS}}/T_{\text{SS}} \quad (3.15)$$

3.5.5 Structures

The structures subsystem inputs the propellant masses and maximum dynamic pressure. It then sizes the propellant tanks to hold the propellant, and the rocket length to hold the tanks. Structural thicknesses are calculated based on loadings conditions. The tanks are sized to hold propellant at the necessary pressures, while the rocket structures are sized to withstand the thrust and drag loads from the point of maximum dynamic pressure, q_{max} . A mass for fasteners and other miscellaneous components is estimated. The first modes of axial and bending vibration are calculated here by treating the rocket as a cylindrical shell, and if the values are too small then the design is considered infeasible.

3.5.6 Systems

The systems module is actually a higher-level routine that handles the function calls of the other subsystems. In the systems subsection the payload mass is calculated by subtracting structural, oxidizer, and fuel masses from the total mass, as according to Eq. (3.16). Since the wet mass was an input, the mass that was not used up as fuel or taken up by structures is the available payload mass.

$$m_p = m - m_{\text{struct}} - m_{\text{ox}} - m_f \quad (3.16)$$

The staging is handled by performing the rocket calculations twice in succession. While performing calculations for the first stage, the second stage is treated as payload, and the calculations take place as they would for a single-stage rocket. After the defined staging altitude is reached, the payload mass is noted and is used as the wet mass for the second stage of the rocket. Thus the model returns to the trajectory subsystem and uses all the ending conditions from the first stage as the beginning conditions for the second stage. The same set of calculations is performed again from the staging altitude to the final altitude, and the remaining payload is output as the final payload mass.

Note that there is little coupling between the subsystems in the model. The only feedback is the second loop of calculations for the second stage as can be seen in Table 3-2, but even this is designed so that the second stage does not impact the first stage. Thus there is no iteration required; this implementation was chosen to allow for faster evaluation of design vectors.

3.5.7 Cost

The cost subsystem calculates the cost for both materials and manufacturing. The material costs are based on material masses and engine mass. The engine is the largest of the material dry masses, and has the highest cost per kilogram, so it makes up the bulk of the material cost. The manufacturing cost is based on seam lengths. The cost parameters include cost per meter of seam and cost per kg of material. These parameters were taken from an external fuel tank model and have been scaled to produce numbers in the expected amounts.^{11,15}

3.5.8 Output

The objective and constraint variables are the outputs of the model. These are the results sent back to the user or optimizer that called the model.

3.6 Benchmarking

The model was benchmarked against five existing rockets from the Delta line in order to verify that the model produced reasonable mass and cost results.¹⁵ These comparisons were done for a launch from Cape Canaveral at 28.5° N latitude to the space station orbit at 407 km altitude, 51.6° inclination. The wet masses, rocket radii, cone angles, initial thrusts, and propellant types from the rockets were each entered into the model. The other flight characteristics were varied until the rocket reached the correct altitude. Then the payload masses and costs from the model were compared to the actual values, and the results are shown in Table 3-3.

Table 3-3. Benchmarking results

Rocket Type	Actual Payload Mass (kg) ¹⁵	Calc. Payload Mass (kg)	% Payload Error	Actual Cost (\$M) ¹⁵	Calc. Cost (\$M)	% Cost Error	Actual m _p /C (kg/\$M) ¹⁵	Calc. m _p /C (kg/\$M)	% m _p /C Error
Delta II 7326-10	2294	2700	17.70	43.5	41.3	-5.06	52.74	65.38	23.97
Delta II 7925-10	4104	3500	-14.72	55	52.5	-4.55	74.62	66.67	-10.66
Delta IV Medium	8501	9990	17.52	72.6	70.1	-3.44	117.09	142.51	21.71
Delta IV Medium+ (4,2)	11455	13800	20.47	98	93.8	-4.29	116.89	147.12	25.87
Delta IV Heavy	21892	24500	11.91	150	162.3	8.20	145.95	150.96	3.43

The calculated payload masses had a 10-20% error with respect to the benchmark actual values. The error was not completely systematic, however, since the results for the Delta II 7925-10 simulation underestimated the payload mass, while the others overestimated. One caveat is that each of these rockets besides the Delta IV Medium uses solid rocket boosters, and the model is not built to handle solid rockets or multiple stages acting in parallel. For the cost estimation, the model was typically low by about 5%. Since the model cost model just works by scaling rocket material cost, manufacturing cost, and engine cost, this suggests that the scaling is simply set slightly too low for the lower range of rockets, but overestimates for larger rockets. Also, the Delta rocket costs used for comparison are the prices to purchase a rocket, so they have overhead and profit margins added on to the actual rocket cost, which this model does not cover. The mass per cost (MPC) errors are of slightly higher magnitude, since the mass and cost errors compound for most cases. This benchmarking analysis suggests that while there are non-negligible errors, the model produces reasonable estimates for payload masses and costs and can be used for comparative testing of optimization methods. This level of fidelity is adequate for use in study of the ISLOCE method, since the most important characteristics in that regard are that the model is complex and responds in an intuitive manner.

3.7 Application of the MOGA to the Model

In order to populate a Pareto front, the multi-objective genetic algorithm described in Section 2.3 was used. This heuristic technique was chosen because the model uses discrete design variables such as material type and propellant type, and genetic algorithms handle discrete variables well. Further, the design space was non-linear,

which makes use of a MOGA appropriate. The two objectives were to maximize J_1 (payload mass) and minimize J_2 (cost); see Eq. (3.1) and (3.2), respectively.

Each optimization run used a population size of 100 members and a run length of 100 generations, for a total of 10,000 design evaluations. The fitness function initialized at a maximum of 1 for each individual. Then it gave a small penalty of 0.01 to each design for each other design that dominated it by having a lower cost and higher payload capability. It also gave a penalty (described below) to each design infeasible due to an ending altitude less than 400 km. The fitness was then squared to increase the gap between the more and less dominated designs. Finally, it gave zero fitness for designs that were otherwise infeasible by being structurally unsound or expending all wet mass as fuel. This fitness value was then used to decide which designs carried on to the next generation of the genetic algorithm. The fitness function for a feasible point is shown in Eq. (3.17).

$$F = \max\{1.0 - 0.01 \cdot n_{\text{dom}} - p(A_{\text{final}}), 0\}^2 \quad (3.17)$$

A variable penalty shown in Eq. (3.18) was used for the altitude constraint. The further the constraint was violated, the more severe the penalty applied. The penalty curve steepened with each generation because a low curve would not penalize the low-altitude designs enough, but a high curve would often cause the entire starting population to have zero fitness. By starting with a low curve and raising it, the MOGA was able to have a diverse population at the beginning, and then focus on feasible designs at the end, in order to find the largest number of interesting designs. Example penalty curves from the 10th and 50th generations are shown in Figure 3-4. The lower curve is the 10th

generation curve, and the higher, stricter curve is the 50th generation. If the penalty is greater than 1, then the fitness bottoms out at 0. This means that a penalty above the dotted line in Figure 3-4 would be equivalent to a design with zero fitness.

$$p(A_{\text{final}}) = [(400 - A_{\text{final}}) / \max\{1, 400 - 4 \cdot \text{generation}\}]^2 \quad (3.18)$$

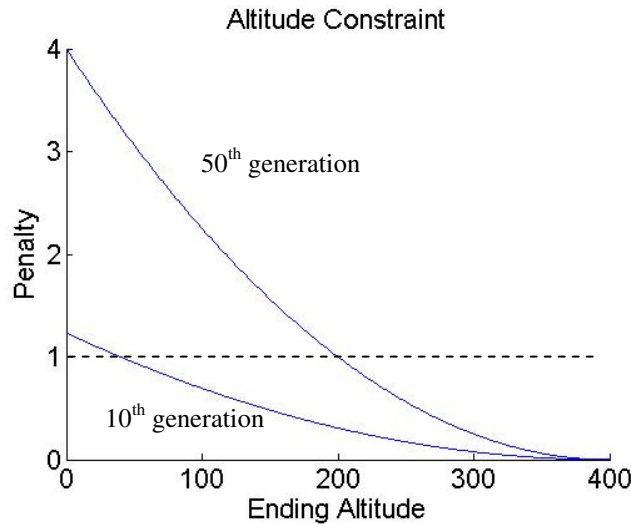


Figure 3-4. Example altitude constraint functions for the 10th and 50th generations

After completing a 100 population, 100 generation run with about a five minute run time, the code would build a Pareto front. When sorting for the Pareto optimal points, the code only considered points that had no penalty for low altitude. From the remaining points it searched for the non-dominated solutions and plotted them.

Below are examples of the output from the genetic algorithm. Figure 3-5 shows all the feasible unpenalized design points from a 100 generation run. Typically of the 10,000 individuals, 2000-4000 would be feasible. Figure 3-6 shows the non-dominated solutions from the first plot. The utopia point is defined as the point which combines the best instances of each objective function into a single point.⁵ For this study, the utopia point

is to the lower right, and for this example has the high payload of 50.7 tons and low cost of 140.2 \$M.

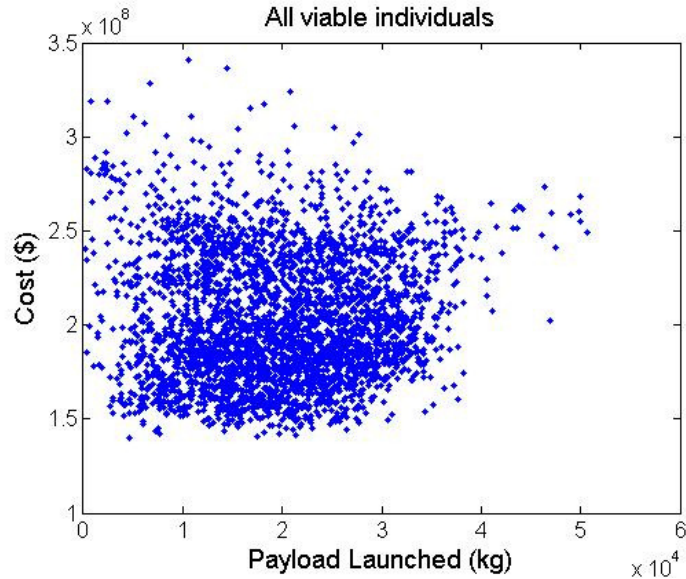


Figure 3-5. All feasible individuals from a MOGA run

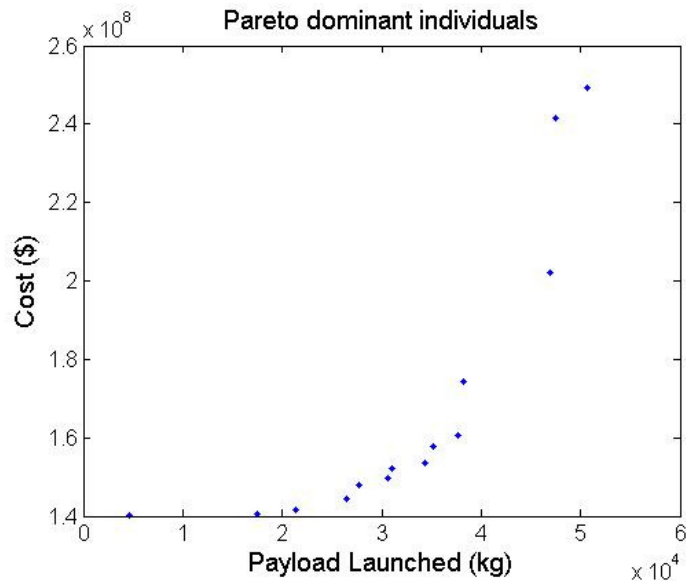


Figure 3-6. Non-dominated individuals

Notice that this Pareto front is not very well distributed and is somewhat jagged. Running the MOGA multiple times would lead to covering different ranges and help fill out the Pareto front.¹⁶ Also, the Pareto fronts made by successive runs would sometimes

be closer or farther from the utopia point. Thus Pareto fronts from multiple optimization runs were combined by collecting the non-dominated individuals from each run, and then comparing them and keeping only the individuals which remain non-dominated across the entire ensemble. The code was run many more times while varying the seeding mechanism, crossover and mutation rates and the plot in Figure 3-7 was produced.

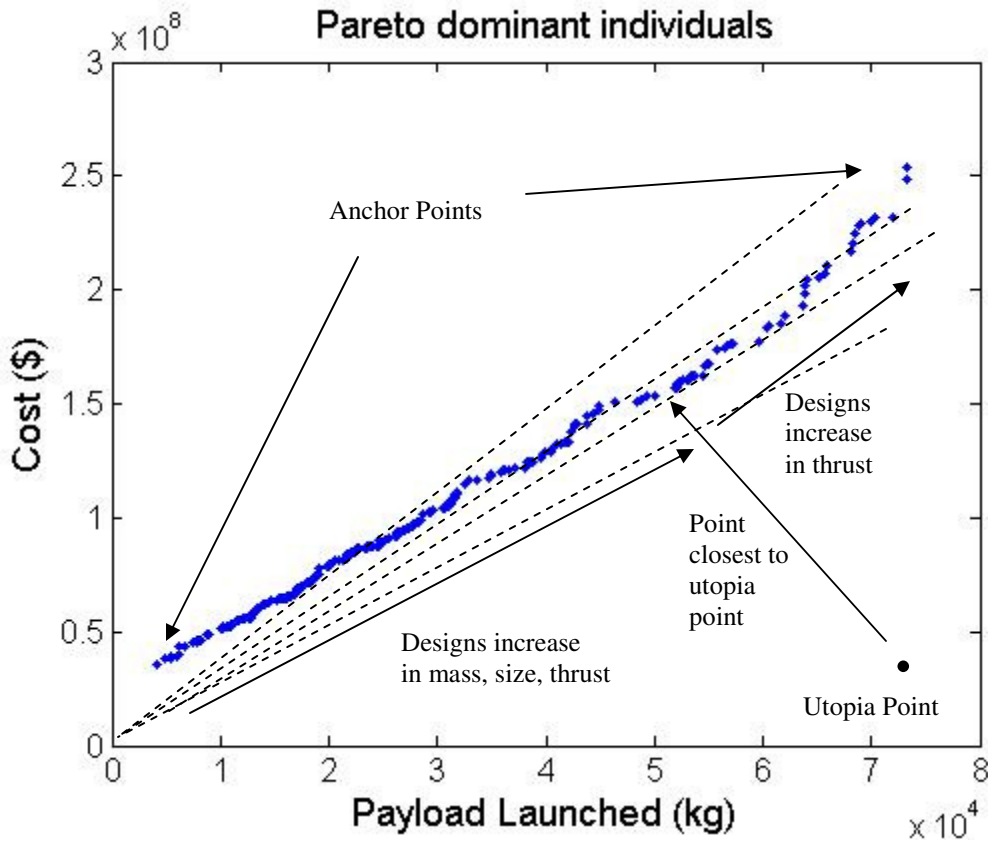


Figure 3-7. Non-dominated points from 1640 MOGA runs with constant C/m_p lines and annotations

After a few hundred runs, the Pareto front becomes well populated, and there are only minor bumps which could either reflect real design changes or be indications that more computation is needed. With 1640 optimization runs the Pareto front is closer to the utopia point of 73.3 tons and 35.5 \$M. The Pareto front is nearly linear, which is likely a result of the cost model being simple and heavily driven by engine size.

In Figure 3-7 we see the low cost and high payload mass anchor points. From those anchor points we can construct a normalized space with vertices (0,0), (1,0), (0,1), and (1,1). (0,0) is the low cost anchor point, (1,1) is the high payload anchor point, and (1,0) is the normalized utopia point. All other points are normalized within this space. We can find the design with the least distance from the utopia point, hereafter referred to as the “best” design. Also plotted are dotted lines of constant cost per payload mass to aid in visualization.

As the designs move up from the lower left point, they increase in mass and thrust. Around two-thirds of the way up, the initial wet mass design vector reaches the upper bound assigned for the optimization. This bound was set arbitrarily, so this problem could be reexamined with greater bounds and analysis on sensitivity to the bounds. Continuing to move upward on the plot, the wet mass cannot increase so payload mass can only be increased by increasing thrust. Having a higher thrust means the ascent is faster and has less fuel consumed due to gravity losses, so more mass is left for payload.

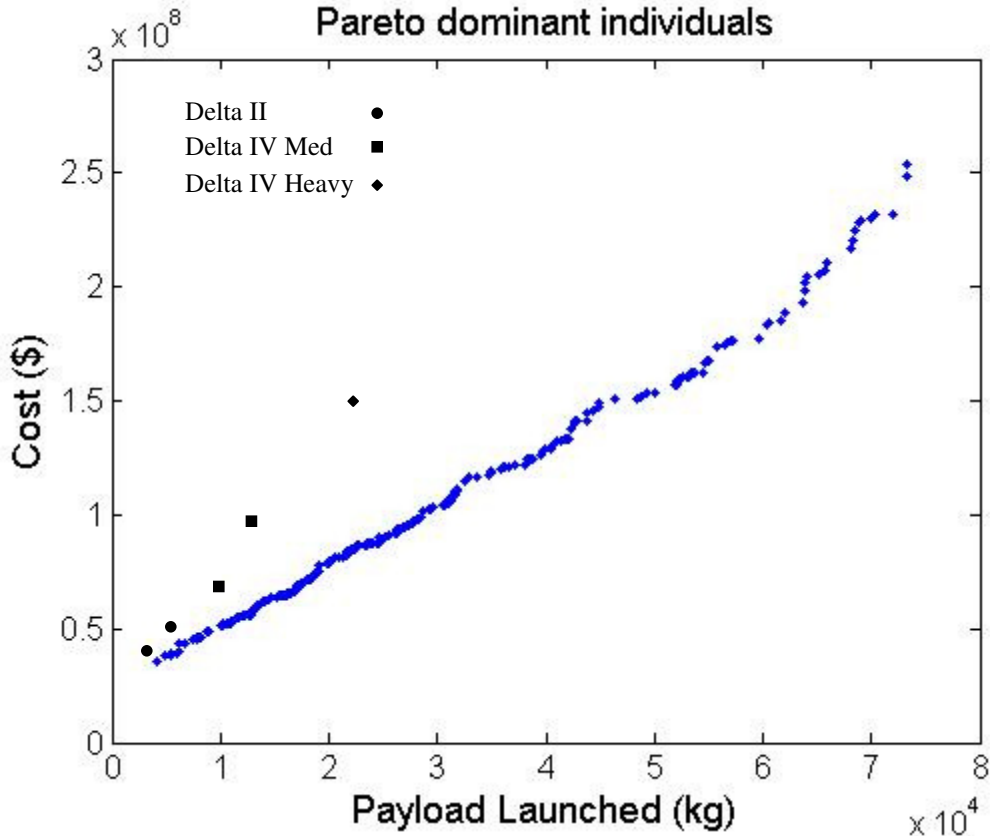


Figure 3-8. Non-dominated points from 1640 MOGA runs with sample rockets plotted¹⁵

In Figure 3-8 we see that the Delta benchmark cases fall along a steeper line of mass/cost. One reason is that the benchmark points are designed for a different inclination and require a plane change maneuver which can be another 3 km/s of delta V, and thus a higher cost per payload slope is expected. The previous benchmarking analysis was a better comparison, which is why the results were closer in that analysis. It is also possible that there are problems in the model, or that the optimization found more efficient designs than the current family of Delta launch vehicles represents.

4 Experiment Description

4.1 Overview

In order to make an empirically supported statement about the features of optimization in concurrent engineering, it was necessary to gather experimental data. This need was met by performing live trials in which participants worked on a realistic design problem. This design problem was to populate a Pareto front for the two-stage liquid rocket model described earlier. The control groups used only the integrated concurrent engineering (ICE) method, while the other groups had an optimizer as a tool, and used the full ISLOCE method. Various metrics could then be used to compare the performances of the design teams with and without real-time optimization.

4.2 Setup

The baseline setup for the control groups used the ICE method implemented with ICEMaker software. The ICEMaker workbooks were created prior to the sessions by coding the MATLAB model in Excel, and linking more complicated calculations with MATLAB where appropriate. Five client workbooks were used to describe the liquid rocket model, and a slightly different model breakdown was used. The bulk of the calculations were done in the Trajectory, Propulsion, and Structures workbooks, then the Cost workbook performed the cost estimation, and finally the Systems workbook collected the data to store and plot. The inputs to the model were distributed among the Trajectory, Propulsion, and Structures workbooks. These served as the design vector, and were manipulated by the client chairs in order to explore different parts of the design space.

For the optimization groups, the same ICEMaker setup was used, and the optimization was run outside of the ICEMaker loop. The multi-objective genetic algorithm (MOGA) described earlier was used. Each 100-generation run of the MOGA took about five minutes, and produced ten to twenty Pareto points. The design vectors for these points could then be used by the design team and entered manually into a list of explored points.

The plan was to run eight to ten sessions of four to five people each, with half of the sessions being control groups, and the other half including optimization. Though there were five ICEMaker client workbooks, multiple workbooks could be run by one person with reasonable workload. The Cost and Systems workbooks in particular had no inputs to the design vector and were expected to be both used by one person. The nominal work breakdown plan is shown in Table 4-1. A session was possible to do with fewer people by having the moderator run the optimizer and/or Cost/Systems workbooks, without providing design input or feedback to the group.

Table 4-1. Nominal work breakdown

Control Group (nominally 4 people)	Optimization Group (nominally 5 people)
Trajectory	Trajectory
Propulsion	Propulsion
Structures	Structures
Cost/Systems	Cost/Systems
	Optimizer

The participants were graduate students from the Massachusetts Institute of Technology. They were recruited from a multidisciplinary optimization class and a space

systems engineering class. This helped standardize their backgrounds, experiences, and interests in systems engineering, design, and optimization. Most students were in the Aeronautics and Astronautics Department, but several were in the Engineering Systems Division or System Design and Management programs.

While the original plan was to run at least eight sessions with four or five students in the session, only seven sessions were actually run, and had from two to four students. The number of sessions was cut because of difficulty in finding participants, and the target number of team members was lowered to three or four. The reason some sessions had as few as two people was that there were last minute cancellations. A summary of the session breakdown is below in Table 4-2.

Table 4-2. Summary of design sessions

Control Groups	Optimization Groups
Group 1, 3/2/6, 4 participants	Group 1, 3/3/6, 4 participants
Group 2, 3/6/6, 4 participants	Group 2, 3/9/6, 4 participants
Group 3, 3/10/6, 2 participants	Group 3, 3/17/6, 3 participants
Group 4, 3/13/6, 2 participants	

4.2.1 Objective

The objective given to each of the design teams was to explore the design space of the liquid rocket model described in Chapter 3 and to populate a Pareto front of non-dominated designs. The teams were encouraged to explore a wide range of point designs, including high-payload, low-cost, and intermediate designs.

4.2.2 Procedure

Each live trial lasted about three hours, with two hours being used for the integrated concurrent engineering design session. Each trial started with a thirty-minute presentation which explained the model, the ICEMaker process, and the session procedure. For the groups that used an optimizer, this presentation also described the role and usage of the optimizer. After the presentation the participants moved to their workstations, where the ICEMaker client workbooks, and MOGA if appropriate, were ready to be run. The next fifteen minutes were spent going over the operation of the client workbooks, and walking through the evaluation of a design point. After the participants were familiar with their tools, the two-hour design session began. At the end of the session, about fifteen minutes were left for discussion of the session.

During the design sessions, the participants manipulated the design vector, and examined the effects on the payload mass and cost of the rocket. The procedure is depicted in Figure 4-1.

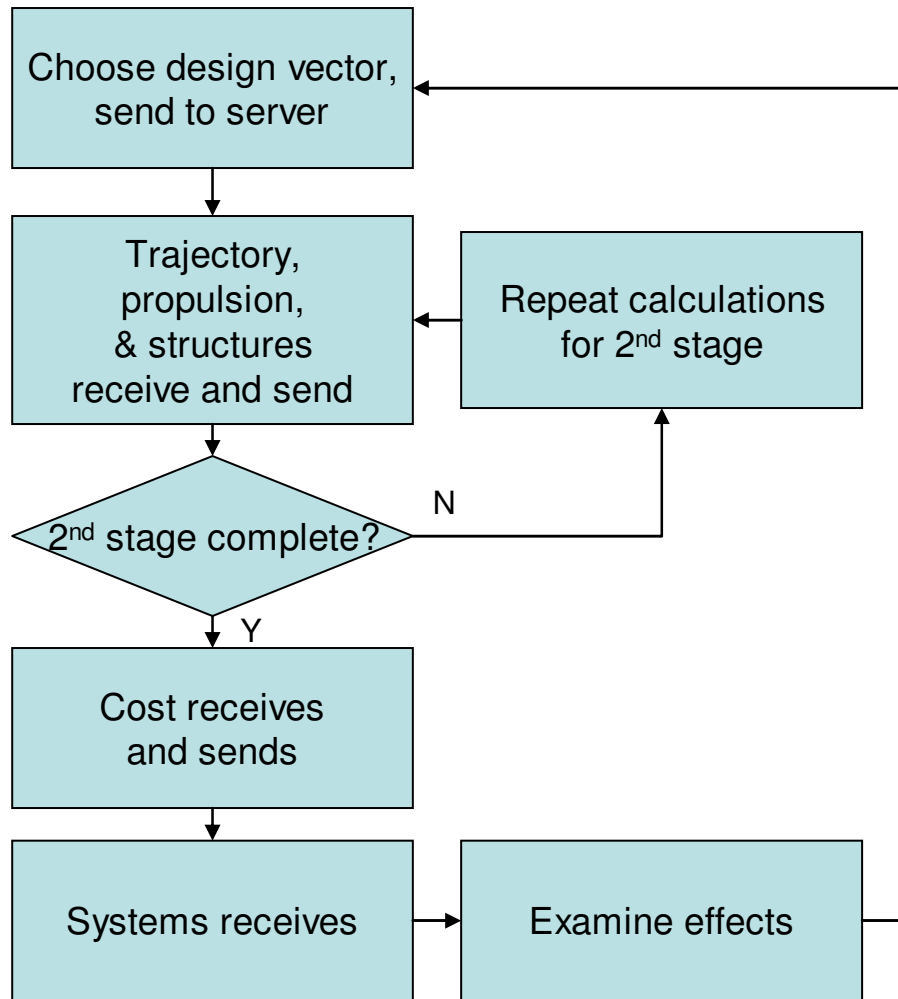


Figure 4-1. Experiment procedure flowchart

The first step in evaluating a point design was to choose the design vector, and update the ICEMaker server with those values. Each of the subsystem clients then evaluated the design point in an order corresponding to Table 3-2. The Trajectory client received inputs from the server and sent the outputs back. This was followed by the Propulsion and Structures clients doing the same. At this point, the calculations for the first stage of the rocket would be complete, and it would be necessary to repeat them for the second stage by rerunning the Trajectory, Propulsion, and Structures models in order. Now the evaluation was completed by running the Cost and Systems clients. The new

point was plotted and recorded in the Systems workbook and then discussion took place on how to vary the design vector for the next evaluation. Once the next design vector was finalized, the procedure was repeated.

The optimization groups had an additional process running in parallel in the background. The optimizer returned results up to every five minutes, and these results could be folded in by deciding during the periodic discussions to take interesting points and evaluate them.

Each group was given the same initial baseline design and the corresponding design vector. This served as a feasible starting point and a foothold to start examining the response of the model to variations of the design variables.

4.3 Metrics

Several metrics were selected to compare the results between sessions. These metrics were developed by Schuman and are described below.²

The bounds of the objective functions are a measure of the extent of the trade space explored during the sessions. For this model, the bounds of the objective function are *maximum payload mass* and *minimum cost* from the design session. These are two metrics which indicate the positions of the anchor points.

The *number of point designs* evaluated during the sessions is a metric for the productivity and the speed at which design points are produced. The *number of non-*

dominated designs shows how many useful points are generated. The ratio of these two metrics, *% non-dominated*, gives a measure of the efficiency of the design session.

The minimum distance of any of the explored points to the utopia point is another useful metric. The utopia point can be the utopia point for the design session, or the utopia point for the combined results from all sessions. The space is normalized by assigning the minimum cost point the location (0,0), the maximum payload point the location (1,1), and the utopia point (1,0). Then the *normalized minimum utopia point distance* is the distance from the utopia point to the closest point evaluated during the session, normalized using the above scheme. The *internal* distance is found by using the utopia point from the specific design session, and the *overall* distance is found by using the best minimum cost and best maximum payload mass from all live-trial design sessions to define the utopia point.

The ranges of the objective functions are the final metrics used in this study. These are the differences between the maximum and minimum values of the objective values of the non-dominated points, and are the *anchor point spread* for *payload* and *cost*.

These metrics allow for comparison between design sessions in many areas, including productivity, efficiency, the performance of the designs, and the degree to which the design space was explored.

5 Results

5.1 Overview

As described in Section 4.2, several design sessions were run using the ICEMaker software, with some groups also using the MOGA as a design tool. The assigned task was to explore a variety of two-stage liquid rocket designs to build a Pareto-front with payload mass and cost as the objective variables. Afterwards, analysis was carried out regarding the performances with respect to the metrics set forth in Section 4.3.

The results from the control and optimization group sessions are described below. The results from one control and one optimization group are discussed in greater detail as examples. The Pareto fronts from the sessions are compared to each other and to optimization results. The metrics are examined and the significance of the differences is analyzed.

5.2 Control Groups

There were four control group live trials carried out. An example of the results from one two-hour design session is shown below in Figure 5-1. These are the points explored by control group 2.

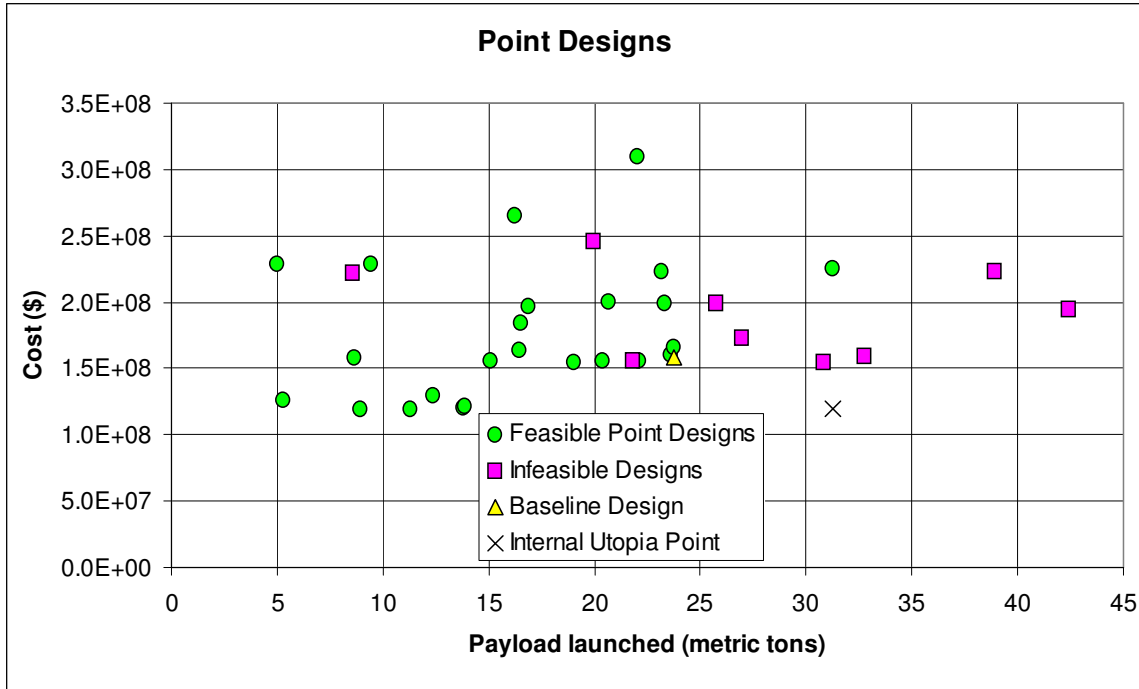


Figure 5-1. Design session results from control group 2

The group investigated a number of design points, including several that were infeasible due to not meeting the constraint of having an ending altitude of at least 400 km. The group was unable to improve upon the baseline by finding a point that dominated it, though it was able to extend the Pareto front into higher payload and lower cost regions. The Pareto front consists of nine non-dominated points, including the baseline point, and the outputs and design variables are listed in Table 5-1. The Pareto fronts for this group and the other three control groups are plotted in Figure 5-2.

Table 5-1. Design variables and objectives for Pareto points from control group 2

Point	m_p (tons)	C (\$)	v_a (Hz)	v_b (Hz)	A_{final} (km)	m_0 (tons)	R_r (m)
Baseline	23.739	1.589E+08	64.1	14.4	418	500.0	4.00
1	8.974	1.199E+08	63.3	7.9	690	550.0	2.25
2	11.278	1.201E+08	60.8	7.3	482	550.0	2.25
3	13.802	1.214E+08	54.5	5.8	436	550.0	2.25
4	13.907	1.216E+08	53.7	5.7	429	560.0	2.25
5	19.063	1.548E+08	55.9	6.8	459	625.0	2.50
6	22.072	1.559E+08	51.5	5.8	409	675.0	2.50
7	23.776	1.665E+08	64.1	14.4	418	500.0	4.00
8	31.241	2.261E+08	46.4	7.5	480	825.0	4.00

Point	θ_c (rad)	T_1 (MN)	T_2 (MN)	T_3 (MN)	T_4 (MN)	T_5 (MN)	α_1 (km)	α_2 (km)
Baseline	0.300	10.00	8.00	4.00	1.00	0.00	200.0	100.0
1	0.700	8.00	8.00	4.00	1.00	0.00	250.0	100.0
2	0.700	8.00	7.00	2.00	1.00	0.00	250.0	100.0
3	0.700	8.00	7.00	2.00	1.00	0.00	250.0	100.0
4	0.700	8.00	7.00	2.00	1.00	0.00	250.0	100.0
5	0.400	10.00	8.00	4.00	2.00	0.00	200.0	100.0
6	0.400	10.00	8.00	4.00	2.00	0.00	200.0	100.0
7	0.300	10.00	8.00	4.00	1.00	0.00	200.0	100.0
8	0.300	13.00	8.00	10.00	3.00	0.00	200.0	100.0

Point	A_{stage}	Prop. 1	Prop 2	Rocket Mat	Tank Mat
Baseline	200.0	LO ₂ /LH ₂	LO ₂ /LH ₂	Ti	Al
1	250.0	NTO/Hydrazine	LO ₂ /LH ₂	Al	Al
2	250.0	NTO/Hydrazine	LO ₂ /LH ₂	Al	Al
3	250.0	LO ₂ /Hydrazine	LO ₂ /LH ₂	Al	Al
4	250.0	LO ₂ /Hydrazine	LO ₂ /LH ₂	Al	Al
5	250.0	LO ₂ /Hydrazine	LO ₂ /LH ₂	Ti	Al
6	250.0	LO ₂ /Hydrazine	LO ₂ /LH ₂	Ti	Al
7	80.0	LO ₂ /LH ₂	LO ₂ /LH ₂	Ti	Ti
8	80.0	LO ₂ /LH ₂	LO ₂ /LH ₂	Ti	Ti

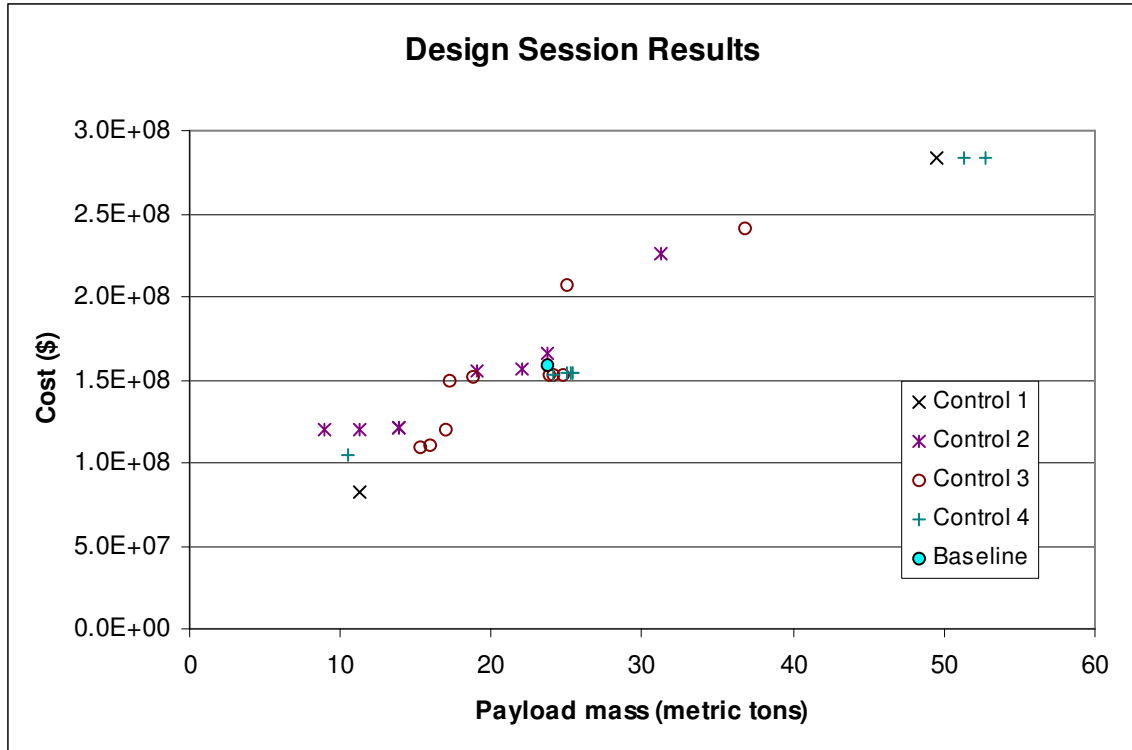


Figure 5-2. Pareto fronts from all control groups

Two of the four groups were able to find designs that dominated the baseline design. The Pareto fronts found by the groups differed in length and population, and some groups spent more time exploring different regions of the design space. The performance metrics for the four control groups are listed in Table 5-2.

Table 5-2. Metric values for the control group design sessions

	Control Groups			
	Group 1	Group 2	Group 3	Group 4
Maximum Payload Mass (tons)	49.46	31.24	36.80	52.77
Minimum Cost (\$)	8.23E+07	1.20E+08	1.09E+08	1.04E+08
# Point Designs	7	24	19	24
# Non-dominated Designs	2	8	10	7
% Non-dominated	28.6%	33.3%	52.6%	29.2%
Normalized Minimum Utopia Point Distance				
<i>Internal</i>	0.773	0.499	0.648	0.704
<i>Overall</i>	0.940	0.940	0.900	0.892
Anchor Point Spread				
<i>Payload Mass (tons)</i>	38.23	22.27	21.48	42.28
<i>Cost (\$)</i>	2.01E+08	1.06E+08	1.32E+08	1.79E+08

There is a fair amount of variability in the performances among the groups. Some groups performed better than others in various metrics or regions of the design space. One of the goals of carrying out multiple design sessions was to mitigate the natural differences into an average.

Most of the groups used a design of experiments (DOE) approach, in which the design variables are varied in a systematic manner to view the system response. This approach had varying levels of success because of the complexity of the design space. Control group 1 performed a simple DOE by setting each design variable to a high value and a low value, but returned mostly infeasible results since they used too large a step size and came up with designs invalid for one reason or another.

5.3 Optimization Groups

There were three optimization group live trials carried out. An example of the results from one two-hour design session is shown below in Figure 5-1. These are the points explored by optimization group 1.

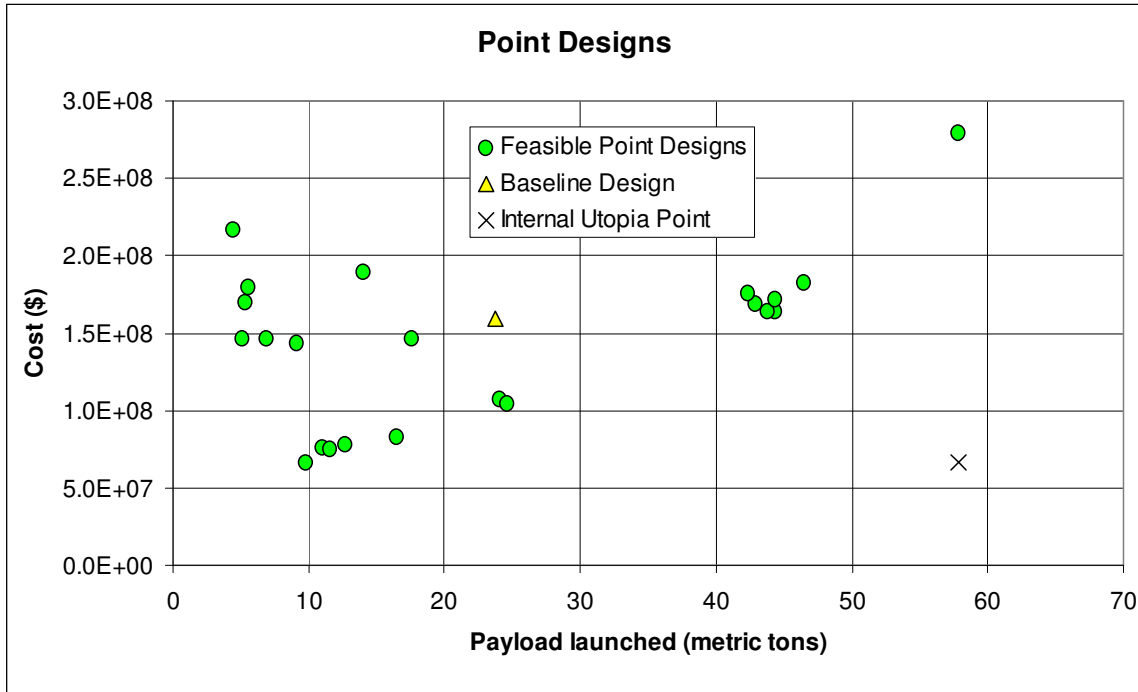


Figure 5-3. Design session results from optimization group 1

There are no infeasible points plotted on this design because the group did not finish the evaluations for any infeasible points. Partway through the investigation of a design point it would become clear whether or not the altitude constraint would be met, and different groups took different approaches as to whether or not to record the point to refer back to later. The group was able to dominate the baseline point, and found a total of eight non-dominated points, described in greater detail in Table 5-3. The Pareto points from the three optimization groups are shown in Figure 5-4.

Table 5-3. Design variables and objectives for Pareto points from optimization group 1

Point	m_p (tons)	C (\$)	v_a (Hz)	v_b (Hz)	A_{final} (km)	m_0 (tons)	R_r (m)
1	9.818	6.634E+07	87.0	13.9	441	269.0	2.10
2	11.620	7.493E+07	52.6	5.1	431	235.0	2.10
3	12.743	7.776E+07	46.3	3.9	413	269.0	2.10
4	16.543	8.270E+07	65.9	8.4	446	430.4	2.23
5	24.661	1.050E+08	42.8	4.0	443	410.0	2.49
6	44.315	1.640E+08	37.8	4.2	409	829.0	3.40
7	46.466	1.831E+08	38.2	4.3	427	829.0	3.40
8	57.843	2.796E+08	47.3	8.9	418	988.0	4.53

Point	θ_c (rad)	T_1 (MN)	T_2 (MN)	T_3 (MN)	T_4 (MN)	T_5 (MN)	α_1 (km)	α_2 (km)
1	0.280	4.05	2.72	3.24	0.10	0.01	127.0	147.0
2	0.280	4.05	3.00	3.00	0.40	0.01	127.0	147.0
3	0.280	4.05	3.00	3.40	0.50	0.01	127.0	147.0
4	0.268	5.21	5.22	4.71	0.10	0.10	9.4	386.0
5	0.178	6.55	5.22	6.44	0.20	0.05	0.0	393.0
6	0.148	11.20	10.00	11.10	0.95	0.07	98.0	188.0
7	0.148	13.00	12.00	11.10	0.95	0.07	98.0	188.0
8	0.175	18.00	19.60	8.10	3.80	1.00	55.0	224.0

Point	A_{stage}	Prop. 1	Prop 2	Rocket Mat	Tank Mat
1	258.0	LO ₂ /Hydrazine	LO ₂ /LH ₂	Al	Al
2	200.0	LO ₂ /LH ₂	LO ₂ /LH ₂	Al	Al
3	200.0	LO ₂ /LH ₂	LO ₂ /LH ₂	Al	Al
4	384.0	LO ₂ /Hydrazine	LO ₂ /LH ₂	Al	Al
5	318.0	LO ₂ /LH ₂	LO ₂ /LH ₂	Al	Al
6	393.0	LO ₂ /LH ₂	LO ₂ /LH ₂	Al	Al
7	393.0	LO ₂ /LH ₂	LO ₂ /LH ₂	Al	Al
8	387.0	LO ₂ /LH ₂	LO ₂ /LH ₂	Al	Ti

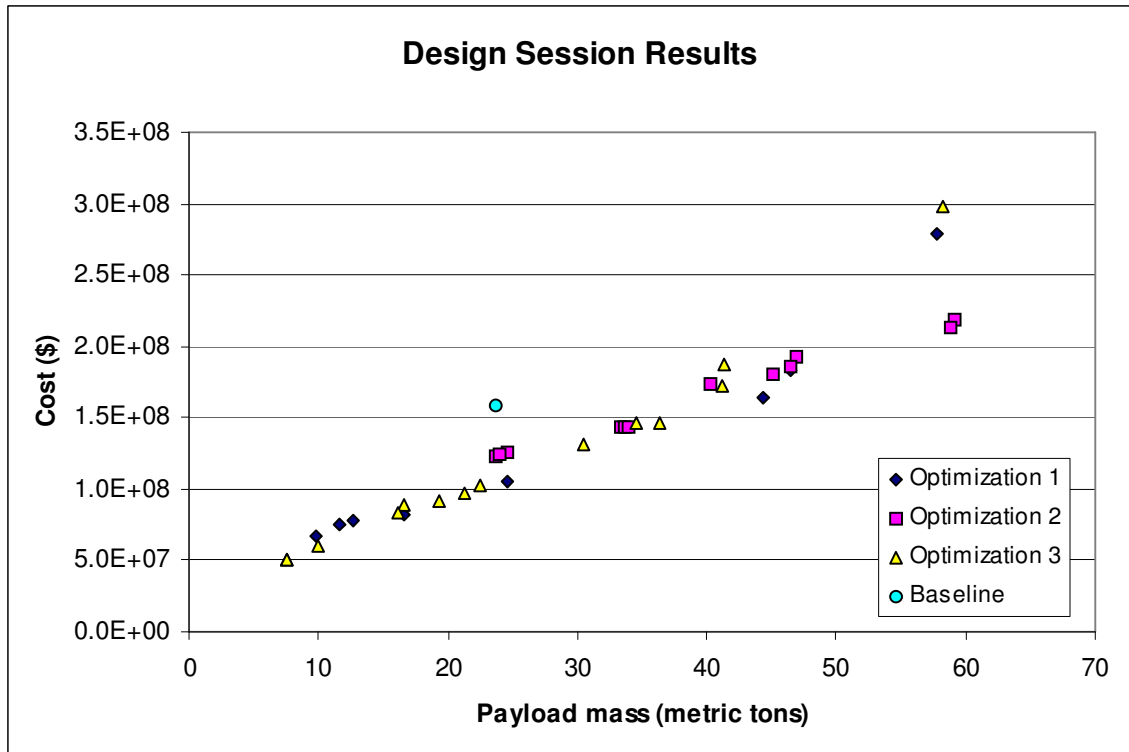


Figure 5-4. Pareto fronts from all optimization groups

The optimization groups all found designs which dominate the baseline design to approximately the same degree. The Pareto fronts of optimization groups 1 and 3 are fairly similar.

For the most part the optimization groups operated in the same ways as the control groups. A few times during the two-hour design sessions they took points from the optimizer and entered them into the ICEMaker models. The optimizer was mostly used to provide good starting points for exploration of different regions of the design space. For this reason, many of the points investigated are clustered together as in Figure 5-3.

The metric results for the optimization groups are shown in Table 5-4.

Table 5-4. Metric values for the optimization group design sessions

	Optimization Groups		
	<i>Group 1</i>	<i>Group 2</i>	<i>Group 3</i>
Maximum Payload Mass (tons)	57.84	59.18	58.24
Minimum Cost (\$)	6.63E+07	1.23E+08	5.10E+07
# Point Designs	22	26	23
# Non-dominated Designs	8	12	14
% Non-dominated	36.4%	46.2%	60.9%
Normalized Minimum Utopia Point Distance			
<i>Internal</i>	0.538	0.720	0.579
<i>Overall</i>	0.731	0.736	0.718
Anchor Point Spread			
<i>Payload Mass (tons)</i>	48.02	35.55	50.70
<i>Cost (\$)</i>	2.13E+08	9.61E+07	2.47E+08

5.4 Comparison

5.4.1 Analysis of Design Points

Figure 5-5 shows a plot with the Pareto fronts from all seven live trials plotted together.

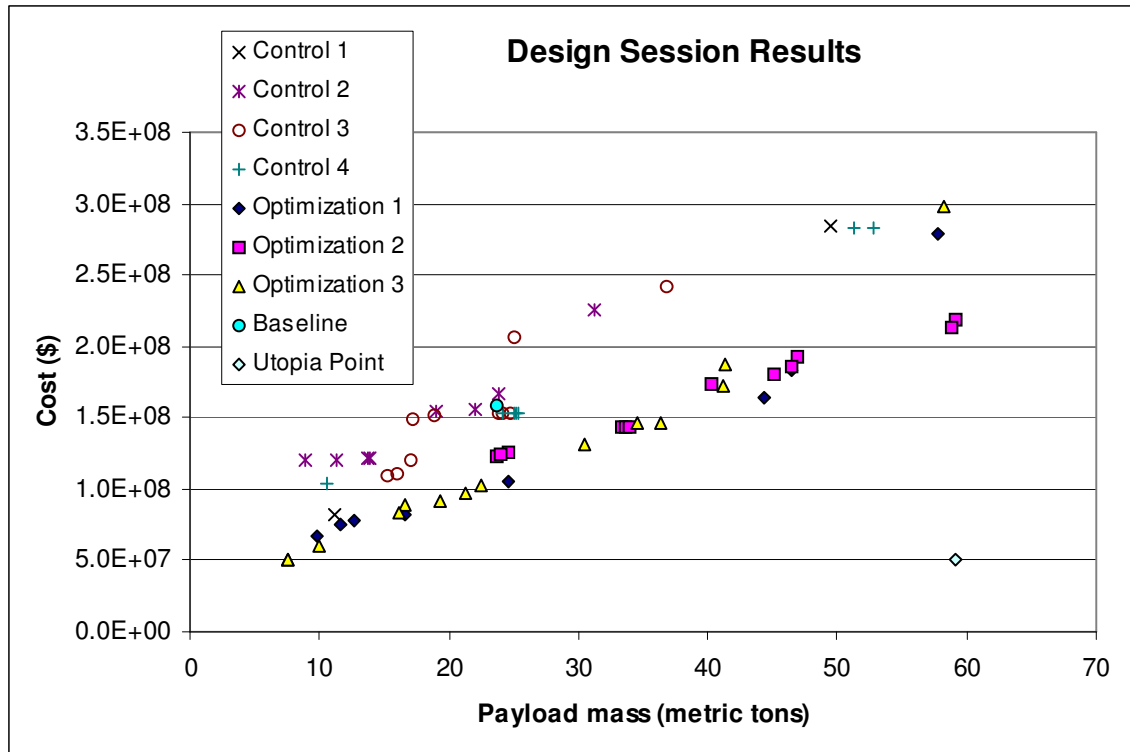


Figure 5-5. Pareto fronts from all design sessions

It is notable that no Pareto point from a control group dominates any Pareto point from an optimization group. Furthermore, every control group Pareto point is dominated by an optimization group Pareto point. If we compare the groups individually rather than overall, then the control groups' points are not always dominated, since the optimization groups had better performances in different regions. The overall utopia point, which takes the low cost of 51 \$M from optimization group 3 and the high payload mass of 59.2 tons from optimization group 2, is also plotted in Figure 5-5.

These results confirm the superior design performance of the optimization groups, given the same amount of design time, as the optimization groups seem to perform at least as well and usually better in regards to the Pareto fronts found. This suggests that optimization combined with ICE is a better design method than ICE alone, though this

will be looked at more rigorously shortly. The results bring up the question of how this process (optimization combined with ICE) compares to optimization alone. In Figure 5-6 MOGA results from offline computation are plotted against the design session results. The MOGA results are the combined Pareto front shown earlier for 1640 optimizer runs.

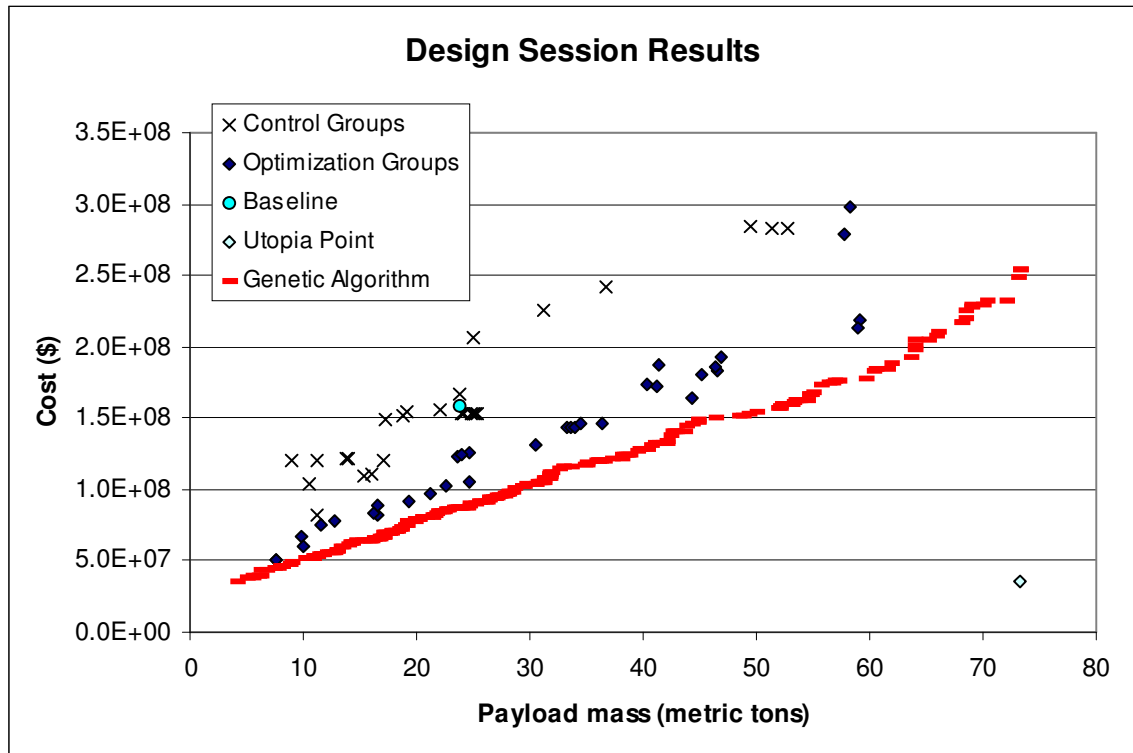


Figure 5-6. Design session results and optimizer results for 1640 runs

The Pareto front from the MOGA dominates all of the design session results, which suggests that an optimizer alone is a stronger tool. However, these results are from allowing the MOGA to run for approximately 130 hours, so it is not a good comparison against a two-hour design session in terms of overall design and computational effort. Additionally the MOGA results would likely not be accepted as easily because humans on the ICE team were not directly involved in generating and negotiating the results. For a better comparison the MOGA was run for two hours and Figure 5-7 was made.

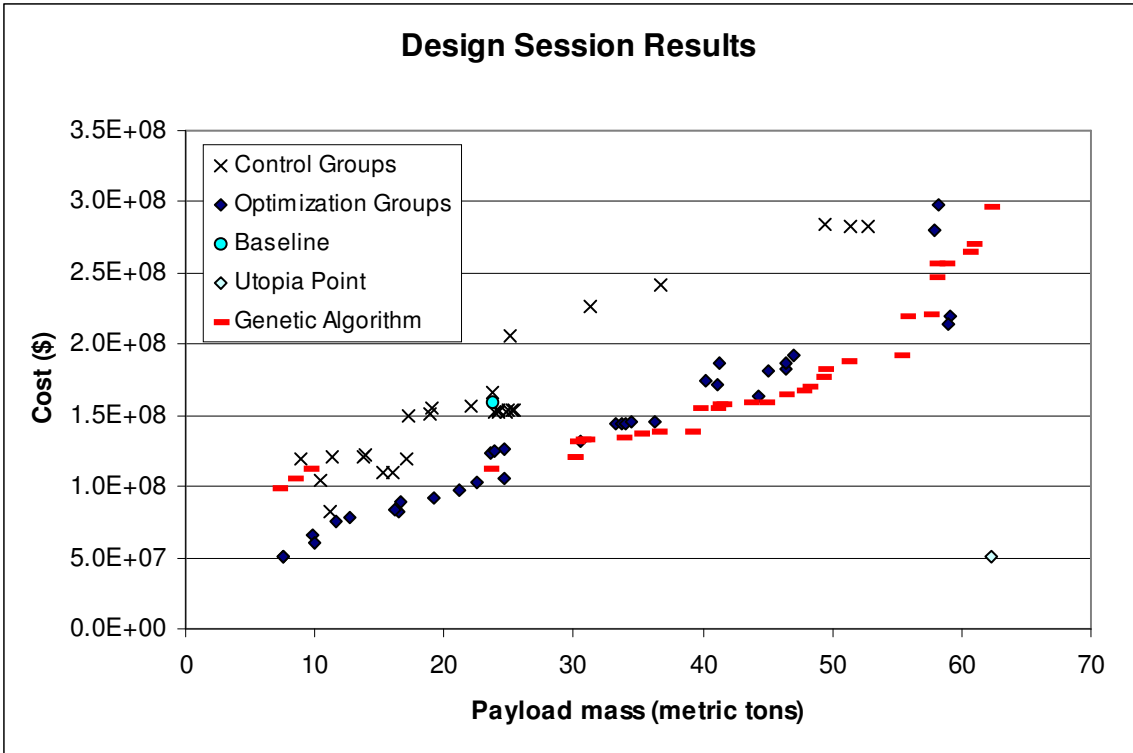


Figure 5-7. Design session results and optimizer results for 2 hour MOGA computation

When the computation time is constrained it is a much more interesting comparison. The optimization group and MOGA points dominate each other at different points along the design space. In the low cost region the MOGA is even dominated by a few control group points.

5.4.2 Analysis of Performance Metrics

The metric values for all seven design sessions are shown together in Table 5-5.

Table 5-5. Metric values from all design sessions

	Control Groups				Optimization Groups		
	Group 1	Group 2	Group 3	Group 4	Group 1	Group 2	Group 3
Maximum Payload Mass (tons)	49.46	31.24	36.80	52.77	57.84	59.18	58.24
Minimum Cost (\$)	8.23E+07	1.20E+08	1.09E+08	1.04E+08	6.63E+07	1.23E+08	5.10E+07
# Point Designs	7	24	19	24	22	26	23
# Non-dominated Designs	2	8	10	7	8	12	14
% Non-dominated	28.6%	33.3%	52.6%	29.2%	36.4%	46.2%	60.9%
Normalized Minimum Utopia Point Distance							
<i>Internal</i>	0.773	0.499	0.648	0.704	0.538	0.720	0.579
<i>Overall</i>	0.940	0.940	0.900	0.892	0.731	0.736	0.718
Anchor Point Spread							
<i>Payload Mass (tons)</i>	38.23	22.27	21.48	42.28	48.02	35.55	50.70
<i>Cost (\$)</i>	2.01E+08	1.06E+08	1.32E+08	1.79E+08	2.13E+08	9.61E+07	2.47E+08

Again, optimization groups do not each perform better than every control group in most of the metrics when doing one-by-one comparisons. Only in the metric of *minimum distance to the overall utopia point* do the optimization groups have constant superiority. This is a very important metric, as it is a measure of the performance of the solutions found. It is also interesting to look at the comparison of metrics between optimization and control groups on an average basis in Table 5-6.

Table 5-6. Average metric values and comparison

	Control Groups	Optimization Groups	% Improvement
Maximum Payload Mass (tons)	42.57	58.42	37.2%
Minimum Cost (\$)	1.04E+08	8.02E+07	22.9%
# Point Designs	18.50	23.67	27.9%
# Non-dominated Designs	6.75	11.33	67.9%
% Non-dominated	35.9%	47.8%	33.0%
Normalized Minimum Utopia Point Distance			
<i>Internal</i>	0.656	0.612	6.7%
<i>Overall</i>	0.918	0.728	20.6%
Anchor Point Spread			
<i>Payload Mass (tons)</i>	31.06	44.76	44.1%
<i>Cost (\$)</i>	1.55E+08	1.85E+08	19.9%

It is notable that with regards to the average metrics the optimization groups perform better in every category. This was an advantage of running multiple sessions, since some of the individual variance that was apparent in Schuman's earlier work was evened out. The metric results from the previous study by Schuman are shown in Table 5-7 and were less definitive, since the optimization group only did better in four of the nine categories.² This is likely partly because only one design session of each type was carried out and the EFT model was of only limited complexity. It is also probable that the increased complexity of the two-stage liquid rocket design problem widened the gap in performance.

Table 5-7. Metric values for EFT design study²

	Control Group	Optimization Group	% Improvement
Maximum Payload Mass (kg)	35948	37181	3.4%
Minimum Cost (\$)	449640	471825	-4.9%
# Point Designs	26	33	26.9%
# Non-dominated Designs	10	7	-30.0%
% Non-dominated	38.5%	21.2%	-44.8%
Normalized Minimum Utopia Point Distance			
<i>Internal</i>	0.617	0.453	26.6%
<i>Overall</i>	0.678	0.563	17.0%
Anchor Point Spread			
<i>Payload (kg)</i>	16727	16633	-0.6%
<i>Cost (\$)</i>	117905	82907	-29.7%

Though the optimization groups performed better in terms of the metrics, it still must be shown to be a statistically significant result. In order to measure the statistical significance a one-sided two-sample t-test was used.¹⁷ This is an appropriate test for two populations with unknown variances, and an assumption is made that they have a normal distribution. A one-sided test was used with the hypothesis that the optimization group performs better. The result from the test is the level of significance for which the null hypothesis is rejected, where the null hypothesis is that the two populations have equal mean. The lower the level of significance the more conclusive the result: a 10% level of significance means the results are 90% likely to not be due to chance and we are 90% confident the hypothesis is true, and a 5% level of significance means the results are 95% likely to not be due to chance and we accept the hypothesis at a 95% level of confidence. Commonly required levels of significance are 10%, 5%, and 0.5%, in order of increasing

strictness. Table 5-8 shows the significance levels for the one-sided two-sample t-test with the hypothesis that the optimization performs better for each metric.

Table 5-8. Significance levels of difference in average performance metrics with one-sided t-test

	Significance Level
Maximum Payload Mass	2.4%
Minimum Cost	15.0%
# Point Designs	16.7%
# Non-dominated Designs	6.3%
% Non-dominated	12.0%
Normalized Minimum Utopia Point Distance	
<i>Internal</i>	31.0%
<i>Overall</i>	0.004%
Anchor Point Spread	
<i>Payload Mass</i>	6.3%
<i>Cost</i>	26.6%

The *normalized minimum distance to the overall utopia point* has a very strong level of significance, allowing for 99.9% confidence that the true mean of the optimization groups is indeed higher. Besides that metric, only the *maximum payload mass* metric allows 95% confidence of improvement. Moving to a 90% requirement of confidence adds the *number of non-dominated designs* and *payload mass anchor point spread* metrics. The remaining metrics are only accepted as having improved at lower levels of confidence.

The improvement in the *distance to the overall utopia point* metric suggests that the biggest advantage of the optimizer is to help improve performance per unit of cost of the

system being designed. In this case, using the optimizer as a design tool helped find rocket designs with simultaneously larger payloads and lower costs. A potential problem with considering only this metric to evaluate performance improvement is that it only looks at the closest distance at the knee of the curve, and the Pareto points at the extremes could be much weaker.

Having a higher number of non-dominated points means that the optimizer also aided the design teams in building a more populated Pareto front. This would give designers more architectures to choose from for further study beyond conceptual design. This metric does not address the issue of how well distributed (i.e. not clustered) the Pareto front is. The metrics regarding anchor points and ranges do address this issue to some extent.

The optimizer also facilitated finding larger payload mass anchor points, and larger spreads in payload mass to give a bigger range of design options. The cost anchor point and cost spread were less significant, however. This may be a peculiarity with the optimizer since the optimizer did not seem to do as well at finding low cost rocket designs for shorter computation times, as shown visually in Figure 5-7.

The number of total designs and percentage of non-dominated designs also expressed lower levels of confidence. The optimizer does not actually speed up the ICEMaker process, but can save time by helping locate feasible regions sooner.

While five of the nine performance metrics did not show improvement significant at the 90% level, this may just be a result of not having enough design sessions. Only

seven total sessions were run due to constraints on number of available participants and time. As the number of trials gets larger, it becomes possible to distinguish finer differences in mean performance.

The performance metrics were compared briefly for the case of optimization groups versus the MOGA. These results are shown in Table 5-9.

Table 5-9. Average optimization group metric values and comparison to 2 hour MOGA

	MOGA	Optimization Groups	% Improvement
Maximum Payload Mass (tons)	62.36	58.42	-6.3%
Minimum Cost (\$)	9.90E+07	8.02E+07	19.0%
# Point Designs	104201	23.67	-100.0%
# Non-dominated Designs	34	11.33	-66.7%
% Non-dominated	0.03%	47.8%	146381.1%
Normalized Minimum Utopia Point Distance			
<i>Internal</i>	0.438	0.612	-39.7%
<i>Overall</i>	0.544	0.737	-35.5%
Anchor Point Spread			
<i>Payload (tons)</i>	55.07	44.76	-18.7%
<i>Cost (\$)</i>	1.97E+08	1.85E+08	-5.9%

The MOGA performed better in most metric categories. The constant calculation led to many more feasible points analyzed, but at a much lower efficiency of discovering non-dominated points. This would be especially relevant if the system model were of higher fidelity and required additional computation. The MOGA found more Pareto points in a wider range, though it was weak in the low cost region. Finally, the MOGA also found a closer design point to the overall utopia point, and this is largely because the MOGA tends to perform better near the middle of the design space.

Therefore, based on computational arguments alone the MOGA is superior to the optimization group which in turn is superior to the control group without optimization. However, as mentioned above, the scalability to complex computationally intensive problems, as well as the poor acceptance of entirely automatically generated answers (MOGA) in engineering practice, make the ISLOCE approach superior to fully automated application of MOGA, as well as to un-augmented system design as practiced by the control group.

6 Conclusions

6.1 Summary

Additional design session trials were done to follow up on ISLOCE work by Schuman.² A two-stage liquid rocket model was developed for use in the study in order to create a more difficult design problem, with the assumption that this would increase the value of using optimization in the ICE process and increase the gap between the control group and the optimization group.

The design sessions were set up with ICEMaker for the ICE implementation and a MOGA to perform the optimization. A total of seven sessions were run with four control groups using only the ICE process, and three groups with access to the MOGA as a tool to augment human decision making.

On average, the groups utilizing optimization performed better in each of the declared performance metrics. There was a significant improvement in objective functions of the designs explored by the optimization groups. The optimization groups also demonstrated a meaningful increase in population size of the Pareto front.

6.2 Future Work

The model constructed was adequate and benchmarked, but had a few issues. The fidelity of the cost model, orbit circularization calculation, and engine modeling in particular could use improvement. Making the model more physically realistic would help make the design session results more representative and validated. A parameterized

CAD model and the ability to attach solid rocket boosters to burn in parallel with the first stage could be included.

The MOGA could be improved as well. Not much time was spent tuning the optimization parameters, because the heuristic nature made it difficult to see what changes helped the MOGA converge or find better results. Also, investigation of the MOGA results showed that the obtained Pareto points could often be improved in payload mass and cost with small adjustments to the design variable. This would suggest that incorporating a gradient-based optimizer into the final step of the MOGA would be beneficial. Having a stronger MOGA would help increase the gap in performance between the optimization groups and control groups, which would strengthen the fundamental conclusions of the thesis.

The metrics for comparison between groups could be augmented by a quantity that measures how well or evenly points are distributed across the Pareto front.

Running additional design sessions could help demonstrate statistically significant improvements for more of the metrics. In particular the design sessions could be run with a variety of engineers from different experience levels and industrial backgrounds (within and outside aerospace) to assess whether previous experience and intuition with rocket design is likely to bias the results. It is suspected that with a large enough number of trials that the optimization group would be shown to be significantly better in every metric relative to the control group. Even if that is not the case, that information would be useful and interesting as well.

Appendix A Design Session Results

A.1 Overview

In order to test the usefulness of including system-level optimization in the ICEMaker process, seven design sessions were carried out. These sessions ran for two hours and had 2-4 student participants. The group compositions, design points, and design point plots for each of the seven groups are shown below.

A.2 Control Group 1

Table A-1. Control group 1 composition

Chair	Subsystem	Program/Major
Participant 1	Trajectory	Engineering Systems Division
Participant 2	Propulsion	System Design & Management
Participant 3	Structures	Mechanical Engineering
Participant 4	Cost, Systems	Engineering Systems Division

Table A-2. Control group 1 feasible design points

Point	m_p (tons)	C (\$)	v_a (Hz)	v_b (Hz)	A_{final} (km)	m_0 (tons)	R_r (m)
1	5.745	1.032E+08	78.9	21.8	675	200.0	4.00
2	8.579	9.354E+07	79.2	22.0	482	200.0	4.00
3	10.455	8.492E+07	88.1	20.4	424	200.0	3.00
4	11.227	8.234E+07	56.9	5.7	425	200.0	2.00
5	2.498	8.468E+07	102.0	18.2	594	300.0	2.00
6	3.505	8.466E+07	102.1	18.3	456	300.0	2.00
7	49.457	2.838E+08	41.3	6.0	436	1000.0	4.00

Point	θ_c (rad)	T_1 (MN)	T_2 (MN)	T_3 (MN)	T_4 (MN)	T_5 (MN)	α_1 (km)	α_2 (km)
1	0.300	5.00	5.00	1.00	1.00	0.10	200.0	100.0
2	0.300	5.00	5.00	1.00	0.10	0.10	200.0	100.0
3	0.300	5.00	5.00	1.00	0.10	0.10	200.0	100.0
4	0.300	5.00	5.00	1.00	0.10	0.10	200.0	100.0
5	0.300	5.00	5.00	1.00	0.50	0.50	300.0	300.0

6	0.300	5.00	5.00	1.00	0.50	0.50	300.0	100.0
7	0.300	20.00	16.00	10.00	2.00	0.10	200.0	100.0
Point	A _{stage}	Prop. 1	Prop. 2	Rocket Mat	Tank Mat	Time		
1	200.0	LO ₂ /LH ₂	LO ₂ /LH ₂	Ti	Al	11:02 AM		
2	200.0	LO ₂ /LH ₂	LO ₂ /LH ₂	Ti	Al	11:05 AM		
3	200.0	LO ₂ /LH ₂	LO ₂ /LH ₂	Ti	Al	11:12 AM		
4	200.0	LO ₂ /LH ₂	LO ₂ /LH ₂	Ti	Al	11:18 AM		
5	300.0	NTO/Hydrazine	NTO/Hydrazine	Ti	Ti	11:48 AM		
6	300.0	NTO/Hydrazine	NTO/Hydrazine	Ti	Ti	12:25 PM		
7	200.0	LO ₂ /LH ₂	LO ₂ /LH ₂	Ti	Al	12:29 PM		

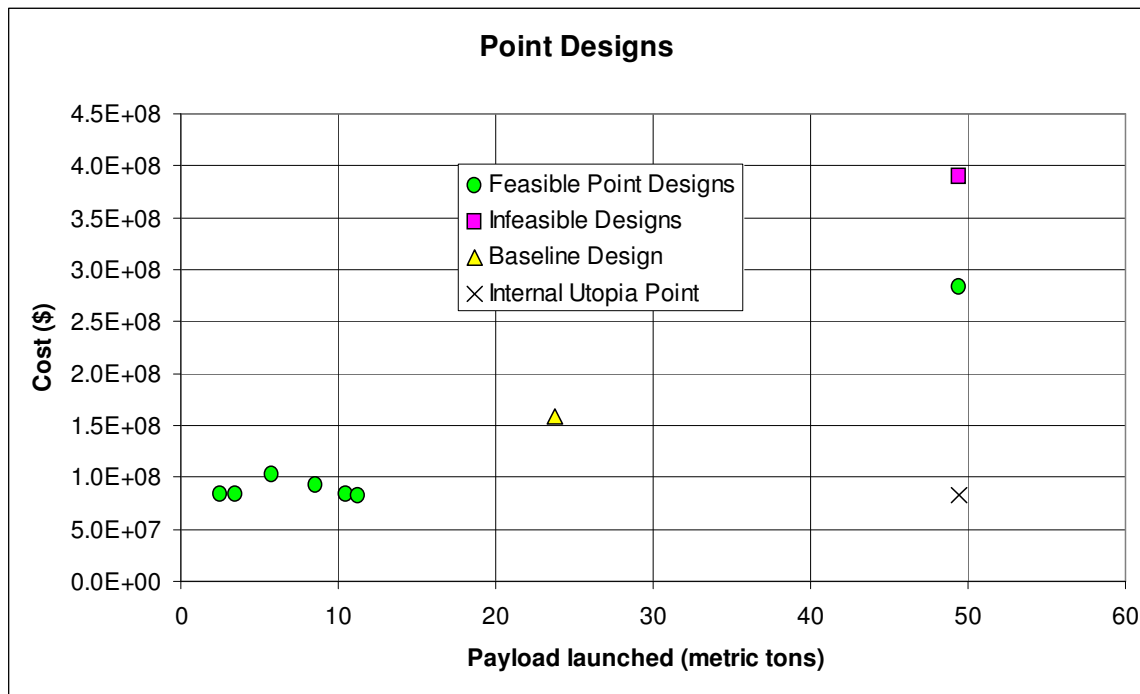


Figure A-1. Control group 1 point designs evaluated

A.3 Control Group 2

Table A-3. Control group 2 composition

Chair	Subsystem	Program/Major
Participant 1	Trajectory	Aeronautics & Astronautics
Participant 2	Propulsion	Aeronautics & Astronautics
Participant 3	Structures	Aeronautics & Astronautics
Participant 4	Cost, Systems	Aeronautics & Astronautics

Table A-4. Control group 2 feasible design points

Point	m_p (tons)	C (\$)	v_a (Hz)	v_b (Hz)	A_{final} (km)	m_0 (tons)	R_r (m)	
1	8.621	1.582E+08	79.6	22.1	514	500.0	4.00	
2	23.620	1.606E+08	64.3	14.4	429	500.0	4.00	
3	23.295	1.994E+08	58.8	12.1	418	600.0	4.00	
4	16.876	1.968E+08	76.1	20.2	482	650.0	4.00	
5	20.648	2.003E+08	71.5	17.9	413	750.0	4.00	
6	15.131	1.567E+08	79.2	22.0	525	500.0	4.00	
7	20.422	1.567E+08	78.4	21.6	412	625.0	4.00	
8	19.063	1.548E+08	55.9	6.8	459	625.0	2.50	
9	22.072	1.559E+08	51.5	5.8	409	675.0	2.50	
10	16.508	1.847E+08	48.6	4.6	503	675.0	2.25	
11	5.279	1.271E+08	69.0	9.4	952	500.0	2.25	
12	8.974	1.199E+08	63.3	7.9	690	550.0	2.25	
13	11.278	1.201E+08	60.8	7.3	482	550.0	2.25	
14	13.802	1.214E+08	54.5	5.8	436	550.0	2.25	
15	13.907	1.216E+08	53.7	5.7	429	560.0	2.25	
16	12.384	1.302E+08	51.4	5.2	452	560.0	2.25	
17	22.057	3.096E+08	53.3	8.1	529	1000.0	3.25	
18	16.233	2.659E+08	55.0	8.6	571	1000.0	3.25	
19	5.028	2.291E+08	54.4	7.0	859	750.0	2.70	
20	9.430	2.294E+08	48.6	5.4	683	750.0	2.60	
21	16.490	1.638E+08	79.2	22.0	502	500.0	4.00	
22	23.776	1.665E+08	64.1	14.4	418	500.0	4.00	
23	31.241	2.261E+08	46.4	7.5	480	825.0	4.00	
24	23.149	2.232E+08	54.9	10.5	621	650.0	4.00	
Point	θ_c (rad)	T_1 (MN)	T_2 (MN)	T_3 (MN)	T_4 (MN)	T_5 (MN)	α_1 (km)	α_2 (km)
1	0.300	10.00	8.00	4.00	1.00	0.00	250.0	75.0
2	0.300	10.00	8.00	4.00	1.00	0.00	250.0	75.0
3	0.300	12.00	8.00	4.00	2.00	0.00	225.0	100.0
4	0.300	12.00	8.00	4.00	2.00	0.00	225.0	100.0
5	0.300	12.00	8.00	4.00	2.00	0.00	225.0	100.0
6	0.300	10.00	8.00	4.00	1.00	0.00	200.0	100.0
7	0.300	10.00	8.00	4.00	1.00	0.00	200.0	100.0
8	0.400	10.00	8.00	4.00	2.00	0.00	200.0	100.0

9	0.400	10.00	8.00	4.00	2.00	0.00	200.0	100.0
10	0.700	13.00	8.00	4.00	2.00	0.00	250.0	100.0
11	0.700	8.00	8.00	4.00	2.00	0.00	250.0	100.0
12	0.700	8.00	8.00	4.00	1.00	0.00	250.0	100.0
13	0.700	8.00	7.00	2.00	1.00	0.00	250.0	100.0
14	0.700	8.00	7.00	2.00	1.00	0.00	250.0	100.0
15	0.700	8.00	7.00	2.00	1.00	0.00	250.0	100.0
16	0.700	8.00	7.00	2.00	1.00	0.00	250.0	100.0
17	0.700	20.00	12.00	6.00	3.00	0.00	250.0	100.0
18	0.700	16.00	10.00	6.00	3.00	0.00	250.0	100.0
19	0.700	12.00	7.00	8.00	3.00	0.00	250.0	100.0
20	0.500	12.00	6.00	8.00	3.00	0.00	250.0	100.0
21	0.300	10.00	8.00	4.00	1.00	0.00	200.0	100.0
22	0.300	10.00	8.00	4.00	1.00	0.00	200.0	100.0
23	0.300	13.00	8.00	10.00	3.00	0.00	200.0	100.0
24	0.300	13.00	8.00	10.00	3.00	0.00	200.0	100.0

Point	A _{stage}	Prop. 1	Prop. 2	Rocket Mat	Tank Mat	Time
1	250.0	LO ₂ /Hydrazine	LO ₂ /Hydrazine	Al	Ti	8:38 AM
2	250.0	LO ₂ /LH ₂	LO ₂ /LH ₂	Al	Ti	8:47 AM
3	150.0	LO ₂ /LH ₂	LO ₂ /LH ₂	Al	Al	9:08 AM
4	150.0	LO ₂ /Kerosene	LO ₂ /LH ₂	Al	Al	9:16 AM
5	150.0	LO ₂ /Kerosene	LO ₂ /LH ₂	Ti	Al	9:19 AM
6	200.0	LO ₂ /Kerosene	LO ₂ /LH ₂	Ti	Al	9:23 AM
7	200.0	LO ₂ /Kerosene	LO ₂ /LH ₂	Ti	Al	9:31 AM
8	250.0	LO ₂ /Hydrazine	LO ₂ /LH ₂	Ti	Al	9:40 AM
9	250.0	LO ₂ /Hydrazine	LO ₂ /LH ₂	Ti	Al	9:45 AM
10	250.0	NTO/Hydrazine	LO ₂ /LH ₂	Al	Al	9:54 AM
11	250.0	NTO/Hydrazine	LO ₂ /LH ₂	Al	Al	9:58 AM
12	250.0	NTO/Hydrazine	LO ₂ /LH ₂	Al	Al	10:03 AM
13	250.0	NTO/Hydrazine	LO ₂ /LH ₂	Al	Al	10:05 AM
14	250.0	LO ₂ /Hydrazine	LO ₂ /LH ₂	Al	Al	10:09 AM
15	250.0	LO ₂ /Hydrazine	LO ₂ /LH ₂	Al	Al	10:12 AM
16	150.0	LO ₂ /Hydrazine	LO ₂ /LH ₂	Al	Al	10:14 AM
17	150.0	LO ₂ /Hydrazine	LO ₂ /LH ₂	Ti	Ti	10:20 AM
18	80.0	LO ₂ /Hydrazine	LO ₂ /LH ₂	Ti	Ti	10:23 AM
19	80.0	LO ₂ /Hydrazine	LO ₂ /LH ₂	Ti	Ti	10:26 AM
20	80.0	LO ₂ /Hydrazine	LO ₂ /LH ₂	Ti	Ti	10:29 AM
21	80.0	LO ₂ /Hydrazine	LO ₂ /LH ₂	Ti	Ti	10:39 AM
22	80.0	LO ₂ /LH ₂	LO ₂ /LH ₂	Ti	Ti	10:40 AM

23	80.0	LO ₂ /LH ₂	LO ₂ /LH ₂	Ti	Ti	10:46 AM
24	80.0	LO ₂ /LH ₂	LO ₂ /LH ₂	Ti	Ti	10:48 AM

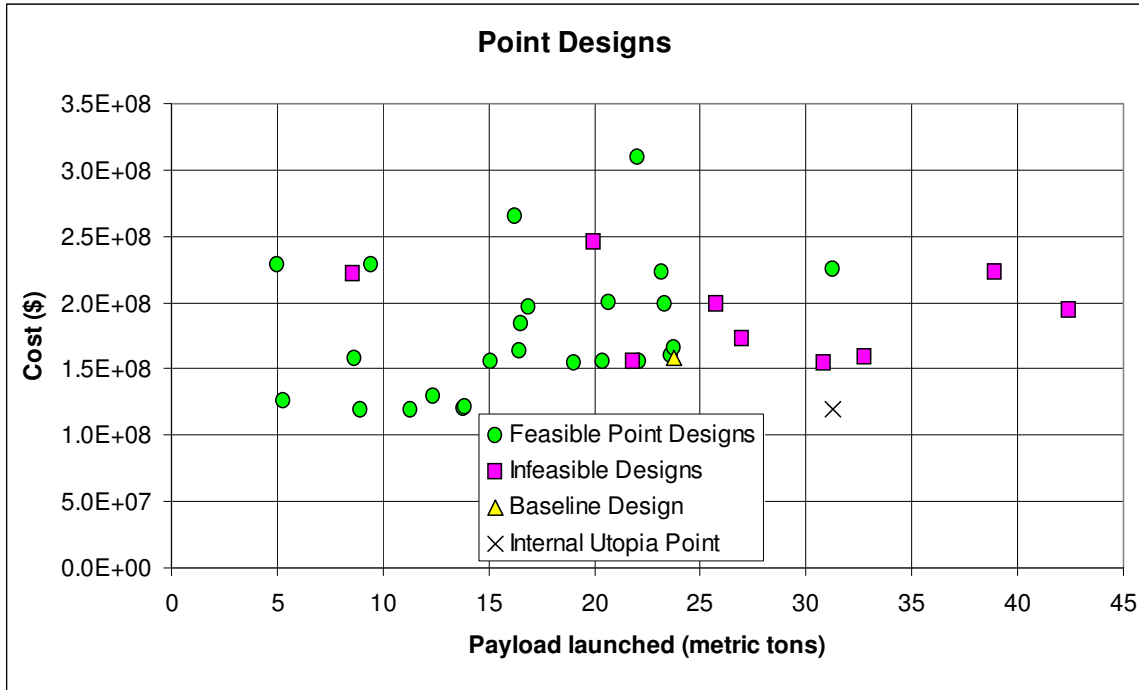


Figure A-2. Control group 2 point designs evaluated

A.4 Control Group 3

Table A-5. Control group 3 composition

Chair	Subsystem	Program/Major
Participant 1	Trajectory	Engineering Systems Division
Participant 2	Propulsion, Structures	Mechanical Engineering
Moderator	Cost, Systems	Aeronautics & Astronautis

Table A-6. Control group 3 feasible design points

Point	m _p (tons)	C (\$)	v _a (Hz)	v _b (Hz)	A _{final} (km)	m ₀ (tons)	R _r (m)
1	17.221	1.581E+08	68.9	16.7	543	400.0	4.00
2	24.757	1.564E+08	58.2	10.4	403	500.0	3.50
3	22.201	1.564E+08	57.6	10.2	429	500.0	3.50

4	24.799	1.634E+08	58.2	10.4	403	500.0	3.50	
5	24.659	1.533E+08	58.4	10.4	403	500.0	3.50	
6	17.190	1.494E+08	87.4	23.3	496	500.0	3.50	
7	15.923	1.497E+08	85.2	22.2	515	500.0	3.50	
8	5.954	1.493E+08	88.8	24.1	539	500.0	3.50	
9	25.026	2.065E+08	59.5	10.8	431	500.0	3.50	
10	17.775	1.748E+08	57.9	10.2	543	500.0	3.50	
11	24.803	1.529E+08	58.4	10.4	401	500.0	3.50	
12	23.903	1.529E+08	58.3	10.4	419	500.0	3.50	
13	24.136	1.529E+08	58.4	10.4	420	500.0	3.50	
14	36.343	2.416E+08	46.6	6.6	435	700.0	3.50	
15	36.797	2.415E+08	46.7	6.7	406	700.0	3.50	
16	18.826	1.515E+08	67.9	14.1	427	400.0	3.50	
17	17.038	1.198E+08	66.6	13.5	480	400.0	3.50	
18	15.312	1.093E+08	65.7	13.2	516	400.0	3.50	
19	15.993	1.103E+08	60.3	11.1	490	450.0	3.50	
Point	θ_c (rad)	T ₁ (MN)	T ₂ (MN)	T ₃ (MN)	T ₄ (MN)	T ₅ (MN)	α_1 (km)	α_2 (km)
1	0.300	10.00	8.00	4.00	1.00	0.00	200.0	100.0
2	0.300	10.00	8.00	4.00	1.00	0.00	200.0	100.0
3	0.400	10.00	8.00	4.00	1.00	0.00	200.0	100.0
4	0.300	10.00	8.00	4.00	1.00	0.00	200.0	100.0
5	0.300	10.00	8.00	4.00	1.00	0.00	200.0	100.0
6	0.300	10.00	8.00	4.00	1.00	0.00	200.0	100.0
7	0.300	10.00	8.00	4.00	1.00	0.00	200.0	100.0
8	0.300	10.00	8.00	4.00	1.00	0.00	200.0	100.0
9	0.300	15.00	8.00	4.00	1.00	0.00	200.0	100.0
10	0.300	10.00	8.00	4.00	3.00	0.00	200.0	100.0
11	0.300	10.00	8.00	4.00	0.96	0.00	200.0	100.0
12	0.300	10.00	8.00	4.00	0.96	0.00	250.0	100.0
13	0.300	10.00	8.00	4.00	0.96	0.00	200.0	200.0
14	0.300	18.00	12.00	6.00	0.96	0.00	200.0	200.0
15	0.300	18.00	10.50	6.00	0.96	0.00	200.0	200.0
16	0.300	10.00	6.00	2.00	1.00	1.00	200.0	200.0
17	0.300	7.00	6.00	4.00	1.00	1.00	200.0	100.0
18	0.300	6.00	6.00	4.00	1.00	1.00	200.0	100.0
19	0.300	6.00	6.00	4.00	1.00	1.00	200.0	100.0
Point	A _{stage}	Prop. 1	Prop. 2	Rocket Mat	Tank Mat	Time		
1	200.0	LO ₂ /LH ₂	LO ₂ /LH ₂	Ti	Al	9:49 AM		
2	200.0	LO ₂ /LH ₂	LO ₂ /LH ₂	Ti	Al	10:02 AM		

3	200.0	LO ₂ /LH ₂	LO ₂ /LH ₂	Ti	Al	10:11 AM
4	200.0	LO ₂ /LH ₂	LO ₂ /LH ₂	Ti	Al	10:14 AM
5	200.0	LO ₂ /LH ₂	LO ₂ /LH ₂	Al	Al	10:17 AM
6	200.0	LO ₂ /Hydrazine	LO ₂ /LH ₂	Al	Al	10:23 AM
7	200.0	LO ₂ /Kerosene	LO ₂ /LH ₂	Al	Al	10:25 AM
8	200.0	NTO/Hydrazine	LO ₂ /LH ₂	Al	Al	10:28 AM
9	200.0	LO ₂ /LH ₂	LO ₂ /LH ₂	Al	Al	10:32 AM
10	200.0	LO ₂ /LH ₂	LO ₂ /LH ₂	Al	Al	10:35 AM
11	200.0	LO ₂ /LH ₂	LO ₂ /LH ₂	Al	Al	10:43 AM
12	200.0	LO ₂ /LH ₂	LO ₂ /LH ₂	Al	Al	10:46 AM
13	200.0	LO ₂ /LH ₂	LO ₂ /LH ₂	Al	Al	10:50 AM
14	200.0	LO ₂ /LH ₂	LO ₂ /LH ₂	Al	Al	11:03 AM
15	200.0	LO ₂ /LH ₂	LO ₂ /LH ₂	Al	Al	11:06 AM
16	200.0	LO ₂ /LH ₂	LO ₂ /LH ₂	Al	Al	11:14 AM
17	200.0	LO ₂ /LH ₂	LO ₂ /LH ₂	Al	Al	11:26 AM
18	200.0	LO ₂ /LH ₂	LO ₂ /LH ₂	Al	Al	11:33 AM
19	200.0	LO ₂ /LH ₂	LO ₂ /LH ₂	Al	Al	11:35 AM

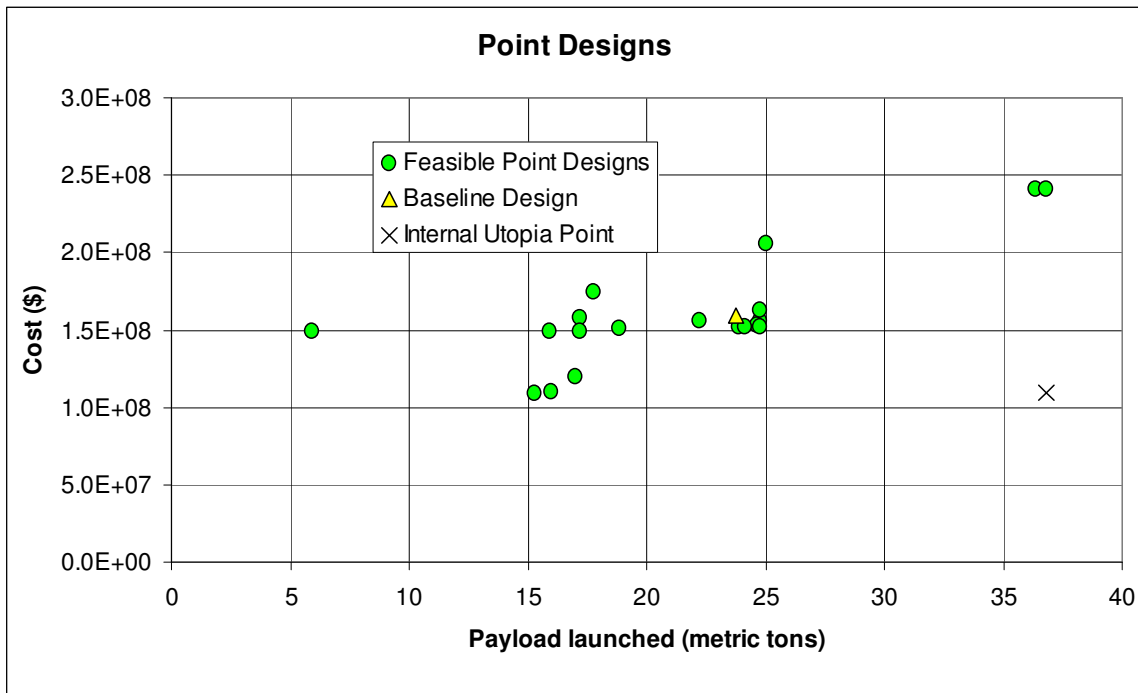


Figure A-3. Control group 3 point designs evaluated

A.5 Control Group 4

Table A-7. Control group 4 composition

Chair	Name	Program/Major
Participant 1	Trajectory	Aeronautics & Astronautics
Participant 2	Propulsion, Structures	Aeronautics & Astronautics
Moderator	Cost, Systems	Aeronautics & Astronautics

Table A-8. Control group 4 feasible design points

Point	m_p (tons)	C (\$)	v_a (Hz)	v_b (Hz)	A_{final} (km)	m_0 (tons)	R_r (m)	
1	22.206	1.590E+08	64.0	14.3	452	500.0	4.00	
2	22.943	1.563E+08	64.0	14.4	445	500.0	4.00	
3	24.969	1.536E+08	64.1	14.4	412	500.0	4.00	
4	23.096	1.590E+08	64.0	14.4	440	500.0	4.00	
5	23.798	1.563E+08	64.1	14.4	435	500.0	4.00	
6	24.487	1.589E+08	64.1	14.4	423	500.0	4.00	
7	24.231	1.536E+08	64.1	14.4	430	500.0	4.00	
8	25.403	1.536E+08	64.1	14.4	402	500.0	4.00	
9	25.245	1.536E+08	64.1	14.4	408	500.0	4.00	
10	22.862	1.432E+08	63.1	14.0	492	500.0	4.00	
11	17.635	1.512E+08	79.2	22.0	474	500.0	4.00	
12	16.191	1.513E+08	79.2	22.0	495	500.0	4.00	
13	14.660	1.513E+08	79.2	22.0	517	500.0	4.00	
14	24.125	1.534E+08	65.1	14.9	421	480.0	4.00	
15	25.303	1.660E+08	57.0	11.4	532	600.0	4.00	
16	47.263	2.896E+08	40.7	5.8	478	1000.0	4.00	
17	51.452	2.897E+08	41.0	5.9	407	1000.0	4.00	
18	48.622	3.029E+08	41.3	6.0	407	1000.0	4.00	
19	52.768	2.831E+08	40.9	5.9	407	1000.0	4.00	
20	51.336	2.831E+08	40.9	5.9	437	1000.0	4.00	
21	7.137	1.363E+08	76.7	20.6	758	250.0	4.00	
22	10.492	1.042E+08	77.3	21.0	428	250.0	4.00	
23	9.281	1.042E+08	77.3	21.0	481	250.0	4.00	
24	9.709	1.094E+08	78.1	21.4	419	250.0	4.00	
Point	θ_c (rad)	T_1 (MN)	T_2 (MN)	T_3 (MN)	T_4 (MN)	T_5 (MN)	α_1 (km)	α_2 (km)
1	0.300	10.00	8.00	4.00	1.00	0.00	300.0	100.0

2	0.300	10.00	8.00	4.00	1.00	0.00	300.0	100.0
3	0.300	10.00	8.00	4.00	1.00	0.00	200.0	100.0
4	0.300	10.00	8.00	4.00	1.00	0.00	200.0	200.0
5	0.300	10.00	8.00	4.00	1.00	0.00	200.0	200.0
6	0.300	10.00	8.00	4.00	1.00	0.00	100.0	300.0
7	0.300	10.00	8.00	4.00	1.00	0.00	250.0	100.0
8	0.300	10.00	8.00	4.00	1.00	0.00	175.0	100.0
9	0.300	10.00	8.00	4.00	1.00	0.00	175.0	125.0
10	0.300	9.00	8.00	6.00	1.00	0.00	175.0	100.0
11	0.300	10.00	8.00	4.00	1.00	0.00	175.0	100.0
12	0.300	10.00	8.00	4.00	1.00	0.00	175.0	100.0
13	0.300	10.00	8.00	4.00	1.00	0.00	175.0	100.0
14	0.300	10.00	8.00	4.00	1.00	0.00	175.0	100.0
15	0.300	10.00	10.00	6.00	3.00	0.00	175.0	100.0
16	0.300	20.00	15.00	10.00	5.00	0.00	175.0	100.0
17	0.200	20.00	15.00	7.00	5.00	0.00	175.0	100.0
18	0.200	20.00	15.00	7.00	5.00	0.00	175.0	100.0
19	0.200	20.00	15.00	7.00	5.00	0.00	175.0	100.0
20	0.200	20.00	15.00	7.00	5.00	0.00	175.0	150.0
21	0.200	7.00	4.00	3.00	2.00	0.00	175.0	150.0
22	0.200	5.00	3.00	2.00	1.00	0.00	175.0	150.0
23	0.200	5.00	3.00	2.00	1.00	0.00	250.0	150.0
24	0.200	5.50	3.00	1.25	1.00	0.00	250.0	150.0
Point	A _{stage}	Prop. 1	Prop. 2	Rocket Mat	Tank Mat	Time		
1	200.0	LO ₂ /LH ₂	LO ₂ /LH ₂	Ti	Al	8:49 AM		
2	250.0	LO ₂ /LH ₂	LO ₂ /LH ₂	Ti	Al	8:51 AM		
3	300.0	LO ₂ /LH ₂	LO ₂ /LH ₂	Ti	Al	8:56 AM		
4	200.0	LO ₂ /LH ₂	LO ₂ /LH ₂	Ti	Al	8:58 AM		
5	250.0	LO ₂ /LH ₂	LO ₂ /LH ₂	Ti	Al	9:00 AM		
6	200.0	LO ₂ /LH ₂	LO ₂ /LH ₂	Ti	Al	9:03 AM		
7	300.0	LO ₂ /LH ₂	LO ₂ /LH ₂	Ti	Al	9:08 AM		
8	300.0	LO ₂ /LH ₂	LO ₂ /LH ₂	Ti	Al	9:11 AM		
9	300.0	LO ₂ /LH ₂	LO ₂ /LH ₂	Ti	Al	9:16 AM		
10	300.0	LO ₂ /LH ₂	LO ₂ /LH ₂	Ti	Al	9:23 AM		
11	300.0	LO ₂ /Hydrazine	LO ₂ /LH ₂	Ti	Al	9:32 AM		
12	300.0	LO ₂ /Kerosene	LO ₂ /LH ₂	Ti	Al	9:34 AM		
13	300.0	NTO/Hydrazine	LO ₂ /LH ₂	Ti	Al	9:35 AM		
14	300.0	LO ₂ /LH ₂	LO ₂ /LH ₂	Ti	Al	9:39 AM		
15	300.0	LO ₂ /LH ₂	LO ₂ /LH ₂	Ti	Al	9:43 AM		

16	300.0	LO ₂ /LH ₂	LO ₂ /LH ₂	Ti	Al	9:47 AM
17	300.0	LO ₂ /LH ₂	LO ₂ /LH ₂	Ti	Al	9:52 AM
18	250.0	LO ₂ /LH ₂	LO ₂ /LH ₂	Ti	Al	9:55 AM
19	325.0	LO ₂ /LH ₂	LO ₂ /LH ₂	Ti	Al	9:57 AM
20	325.0	LO ₂ /LH ₂	LO ₂ /LH ₂	Ti	Al	10:10 AM
21	200.0	LO ₂ /LH ₂	LO ₂ /LH ₂	Ti	Al	10:29 AM
22	200.0	LO ₂ /LH ₂	LO ₂ /LH ₂	Ti	Al	10:31 AM
23	200.0	LO ₂ /LH ₂	LO ₂ /LH ₂	Ti	Al	10:34 AM
24	200.0	LO ₂ /LH ₂	LO ₂ /LH ₂	Ti	Al	10:41 AM

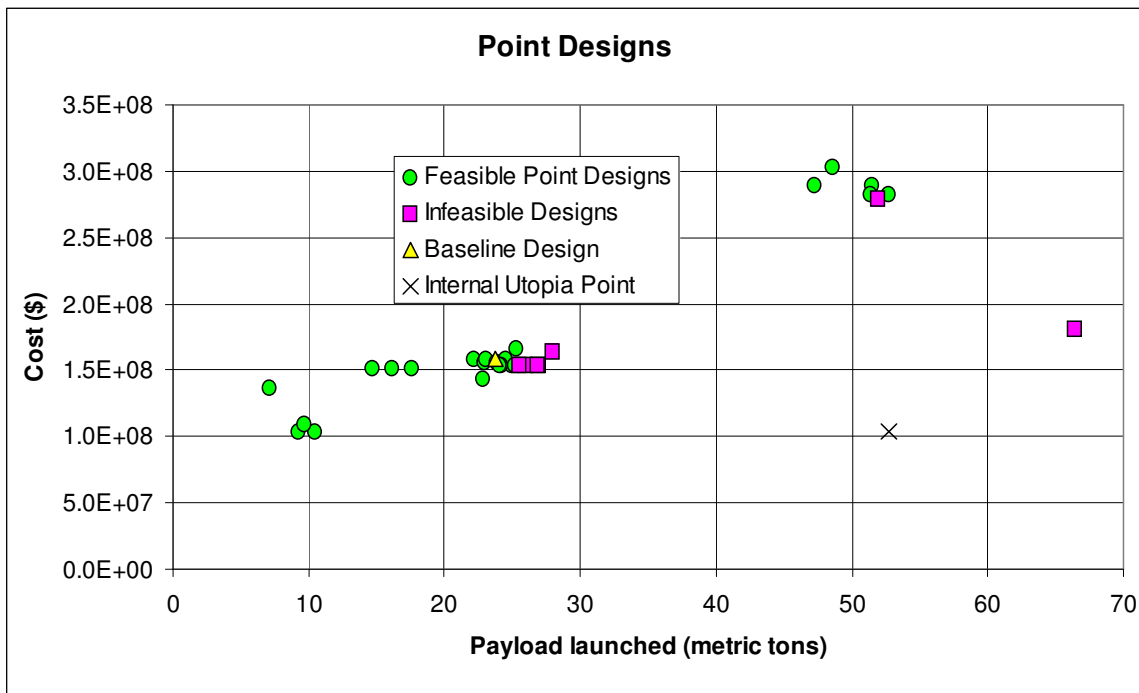


Figure A-4. Control group 4 point designs evaluated

A.6 Optimization Group 1

Table A-9. Optimization group 1 composition

Chair	Subsystem	Program/Major
Participant 1	Trajectory	Engineering Systems Division
Participant 2	Propulsion	Aeronautics & Astronautics
Participant 3	Structures	Aeronautics & Astronautics
Participant 4	Cost, Systems	Aeronautics & Astronautics
Moderator	Optimizer	Aeronautics & Astronautics

Table A-10. Optimization group 1 feasible design points

Point	m_p (tons)	C (\$)	v_a (Hz)	v_b (Hz)	A_{final} (km)	m_0 (tons)	R_r (m)
1	5.337	1.696E+08	64.3	14.5	580	500.0	4.00
2	5.146	1.468E+08	79.2	22.0	528	600.0	4.00
3	6.895	1.468E+08	79.2	22.0	434	600.0	4.00
4	17.646	1.468E+08	79.2	22.0	433	600.0	4.00
5	57.843	2.796E+08	47.3	8.9	418	988.0	4.53
6	44.315	1.640E+08	37.8	4.2	409	829.0	3.40
7	9.150	1.433E+08	72.8	9.9	1027	386.0	2.14
8	13.990	1.899E+08	68.4	13.5	453	800.0	3.30
9	5.557	1.799E+08	71.4	9.5	867	386.0	2.14
10	4.492	2.165E+08	57.6	6.2	503	386.0	2.14
11	46.466	1.831E+08	38.2	4.3	427	829.0	3.40
12	43.806	1.642E+08	43.6	6.3	413	829.0	3.80
13	44.387	1.723E+08	37.8	4.2	409	829.0	3.40
14	42.926	1.690E+08	37.5	4.2	436	829.0	3.40
15	42.391	1.759E+08	34.6	3.6	473	900.0	3.40
16	9.818	6.634E+07	87.0	13.9	441	269.0	2.10
17	12.743	7.776E+07	46.3	3.9	413	269.0	2.10
18	11.031	7.604E+07	52.5	5.0	479	235.0	2.10
19	11.620	7.493E+07	52.6	5.1	431	235.0	2.10
20	16.543	8.270E+07	65.9	8.4	446	430.4	2.23
21	24.057	1.076E+08	42.8	4.0	466	410.0	2.49
22	24.661	1.050E+08	42.8	4.0	443	410.0	2.49

Point	θ_c (rad)	T_1 (MN)	T_2 (MN)	T_3 (MN)	T_4 (MN)	T_5 (MN)	α_1 (km)	α_2 (km)
1	0.300	10.00	8.00	5.00	2.00	0.00	200.0	200.0
2	0.200	7.00	8.00	5.00	2.00	0.00	100.0	200.0
3	0.200	7.00	8.00	5.00	2.00	0.00	75.0	150.0
4	0.200	7.00	8.00	5.00	2.00	0.00	75.0	150.0
5	0.175	18.00	19.60	8.10	3.80	1.00	55.0	224.0
6	0.148	11.20	10.00	11.10	0.95	0.07	98.0	188.0
7	0.199	10.20	2.20	10.40	1.20	0.06	357.0	393.0
8	0.150	10.20	2.20	10.40	1.20	0.06	100.0	150.0
9	0.199	10.20	2.20	10.40	1.20	0.06	100.0	150.0
10	0.199	10.20	2.20	7.00	1.20	0.06	75.0	125.0

11	0.148	13.00	12.00	11.10	0.95	0.07	98.0	188.0
12	0.160	11.20	10.00	11.10	0.95	0.07	98.0	188.0
13	0.148	11.20	10.00	11.10	0.95	0.07	98.0	188.0
14	0.148	11.20	10.00	11.10	2.00	0.50	98.0	188.0
15	0.148	11.20	10.00	11.10	4.00	0.07	110.0	188.0
16	0.280	4.05	2.72	3.24	0.10	0.01	127.0	147.0
17	0.280	4.05	3.00	3.40	0.50	0.01	127.0	147.0
18	0.280	4.05	3.00	3.40	0.50	0.01	127.0	147.0
19	0.280	4.05	3.00	3.00	0.40	0.01	127.0	147.0
20	0.268	5.21	5.22	4.71	0.10	0.10	9.4	386.0
21	0.178	6.55	5.22	6.44	0.52	0.24	0.0	393.0
22	0.178	6.55	5.22	6.44	0.20	0.05	0.0	393.0
Point	A _{stage}	Prop. 1	Prop. 2	Rocket Mat	Tank Mat	Time		
1	200.0	LO ₂ /LH ₂	NTO/Hydrazine	Ti	Al	9:40 AM		
2	200.0	LO ₂ /Hydrazine	NTO/Hydrazine	Ti	Al	9:47 AM		
3	200.0	LO ₂ /Hydrazine	NTO/Hydrazine	Ti	Al	9:58 AM		
4	200.0	LO ₂ /Hydrazine	LO ₂ /LH ₂	Ti	Al	10:02 AM		
5	387.0	LO ₂ /LH ₂	LO ₂ /LH ₂	Al	Ti	10:17 AM		
6	393.0	LO ₂ /LH ₂	LO ₂ /LH ₂	Al	Al	10:23 AM		
7	394.0	LO ₂ /Hydrazine	LO ₂ /LH ₂	Al	Ti	10:30 AM		
8	175.0	LO ₂ /Hydrazine	LO ₂ /LH ₂	Al	Ti	10:34 AM		
9	175.0	LO ₂ /Hydrazine	LO ₂ /LH ₂	Al	Ti	10:37 AM		
10	100.0	LO ₂ /Hydrazine	LO ₂ /LH ₂	Al	Ti	10:42 AM		
11	393.0	LO ₂ /LH ₂	LO ₂ /LH ₂	Al	Al	10:49 AM		
12	393.0	LO ₂ /LH ₂	LO ₂ /LH ₂	Al	Al	10:52 AM		
13	393.0	LO ₂ /LH ₂	LO ₂ /LH ₂	Al	Ti	10:56 AM		
14	393.0	LO ₂ /LH ₂	LO ₂ /LH ₂	Al	Al	10:59 AM		
15	350.0	LO ₂ /LH ₂	LO ₂ /LH ₂	Al	Al	11:07 AM		
16	258.0	LO ₂ /Hydrazine	LO ₂ /LH ₂	Al	Al	11:12 AM		
17	200.0	LO ₂ /LH ₂	LO ₂ /LH ₂	Al	Al	11:22 AM		
18	200.0	LO ₂ /LH ₂	LO ₂ /LH ₂	Al	Al	11:26 AM		
19	200.0	LO ₂ /LH ₂	LO ₂ /LH ₂	Al	Al	11:29 AM		
20	384.0	LO ₂ /Hydrazine	LO ₂ /LH ₂	Al	Al	11:37 AM		
21	318.0	LO ₂ /LH ₂	LO ₂ /LH ₂	Al	Al	11:41 AM		
22	318.0	LO ₂ /LH ₂	LO ₂ /LH ₂	Al	Al	11:46 AM		

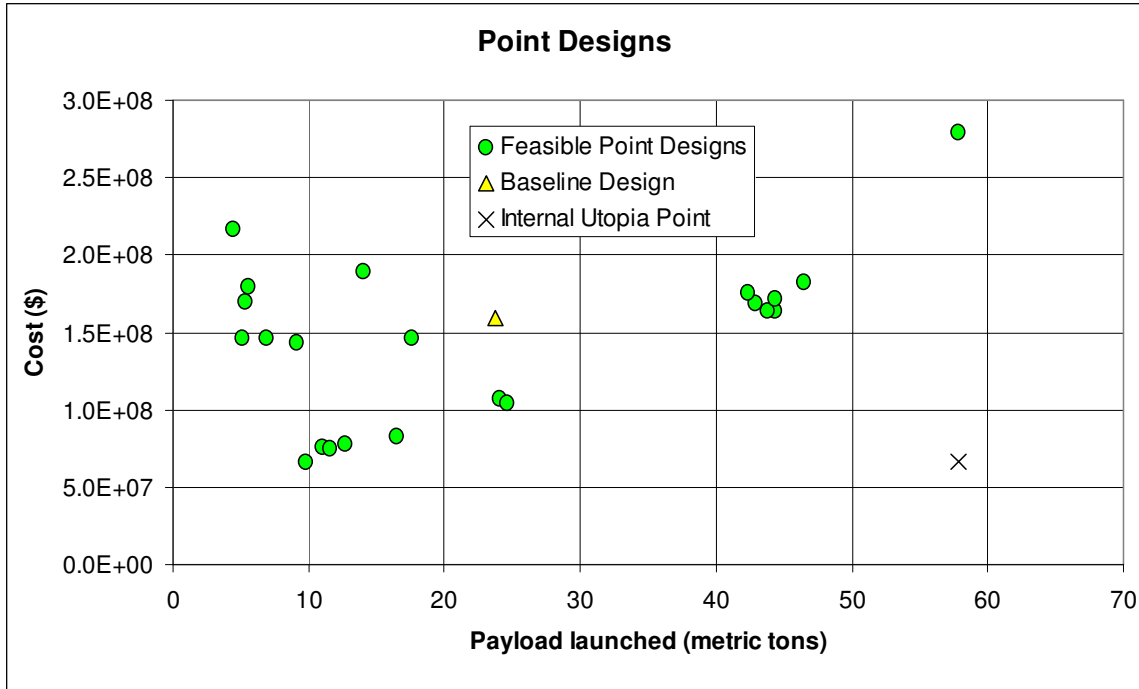


Figure A-5. Optimization group 1 point designs evaluated

A.7 Optimization Group 2

Table A-11. Optimization group 2 composition

Chair	Subsystem	Program/Major
Participant 1	Trajectory	Aeronautics & Astronautics
Participant 2	Propulsion	System Design & Management
Participant 3	Structures	Architecture
Participant 4	Cost, Systems	Aeronautics & Astronautics
Moderator	Optimizer	Aeronautics & Astronautics

Table A-12. Optimization group 2 feasible design points

Point	m_p (tons)	C (\$)	v_a (Hz)	v_b (Hz)	A_{final} (km)	m_0 (tons)	R_r (m)
1	0.798	2.562E+08	59.9	12.6	1133	550.0	4.00
2	23.600	1.590E+08	64.1	14.4	424	500.0	4.00
3	40.279	1.741E+08	50.8	10.3	436	882.0	4.58
4	25.680	1.708E+08	68.7	18.8	559	882.0	4.58
5	28.026	1.705E+08	69.5	19.3	531	882.0	4.58
6	29.480	1.763E+08	44.6	7.9	500	1000.0	4.58

7	46.888	1.993E+08	47.0	8.8	442	1000.0	4.58	
8	47.307	2.296E+08	47.3	8.9	516	1000.0	4.58	
9	46.979	1.925E+08	47.0	8.8	420	1000.0	4.58	
10	46.426	1.863E+08	46.9	8.8	406	1000.0	4.58	
11	46.641	1.998E+08	46.7	8.7	406	1000.0	4.58	
12	45.603	1.883E+08	50.4	11.1	411	1000.0	5.00	
13	46.105	1.873E+08	49.0	10.0	406	1000.0	4.80	
14	45.107	1.809E+08	46.9	8.8	401	1000.0	4.60	
15	31.668	1.508E+08	40.3	4.0	511	549.0	2.80	
16	31.926	1.438E+08	40.2	4.0	480	549.0	2.80	
17	31.848	1.442E+08	40.2	4.0	480	549.0	2.80	
18	33.330	1.437E+08	40.3	4.0	426	549.0	2.80	
19	33.695	1.437E+08	40.3	4.0	411	549.0	2.80	
20	33.998	1.437E+08	40.3	4.0	402	549.0	2.80	
21	33.616	1.444E+08	53.7	8.8	406	549.0	3.50	
22	24.620	1.264E+08	40.1	4.1	536	572.0	2.90	
23	23.631	1.231E+08	39.9	4.0	527	572.0	2.90	
24	23.963	1.245E+08	37.0	3.5	509	620.0	2.90	
25	59.184	2.192E+08	34.2	3.6	405	996.0	3.50	
26	58.898	2.139E+08	34.2	3.6	403	996.0	3.50	
Point	θ_c (rad)	T_1 (MN)	T_2 (MN)	T_3 (MN)	T_4 (MN)	T_5 (MN)	α_1 (km)	α_2 (km)
1	0.300	10.00	8.00	4.00	10.00	0.00	200.0	80.0
2	0.300	10.00	8.00	4.00	1.00	0.00	200.0	120.0
3	0.190	11.40	11.40	10.40	0.80	0.23	252.0	175.0
4	0.190	11.40	11.40	10.40	0.80	0.23	252.0	175.0
5	0.190	11.40	11.40	10.40	0.80	0.23	252.0	175.0
6	0.190	11.40	11.40	10.40	0.80	0.23	252.0	175.0
7	0.190	13.50	13.50	12.00	1.00	0.30	252.0	175.0
8	0.190	16.00	16.00	14.00	1.50	0.40	252.0	175.0
9	0.190	13.00	13.00	11.50	0.80	0.25	252.0	175.0
10	0.190	12.50	12.50	11.00	0.70	0.20	252.0	175.0
11	0.190	12.50	12.50	11.00	0.70	0.20	252.0	175.0
12	0.190	12.50	12.50	11.00	0.70	0.20	252.0	175.0
13	0.190	12.50	12.50	11.00	0.70	0.20	252.0	175.0
14	0.190	12.00	12.00	10.50	0.68	0.18	252.0	175.0
15	0.180	10.20	10.30	9.50	0.91	0.30	75.0	138.0
16	0.180	9.50	9.70	9.00	0.78	0.25	75.0	138.0
17	0.180	9.50	9.70	9.00	0.78	0.25	75.0	138.0
18	0.180	9.50	9.70	9.00	0.78	0.25	75.0	100.0

19	0.180	9.50	9.70	9.00	0.78	0.25	75.0	90.0
20	0.180	9.50	9.70	9.00	0.78	0.25	73.0	90.0
21	0.180	9.50	9.70	9.00	0.78	0.25	73.0	90.0
22	0.170	6.80	8.00	8.10	0.80	0.08	173.0	379.0
23	0.170	6.40	7.60	7.80	0.76	0.07	173.0	379.0
24	0.170	6.40	7.60	7.80	0.76	0.07	173.0	379.0
25	0.100	16.00	14.30	13.20	0.50	0.05	65.0	233.0
26	0.100	15.50	14.30	13.20	0.50	0.05	65.0	233.0
Point	A _{stage}	Prop. 1	Prop. 2	Rocket Mat	Tank Mat	Time		
1	200.0	LO ₂ /LH ₂	LO ₂ /LH ₂	Ti	Al	10:54 AM		
2	200.0	LO ₂ /LH ₂	LO ₂ /LH ₂	Ti	Al	11:03 AM		
3	283.0	LO ₂ /LH ₂	LO ₂ /LH ₂	Al	Al	11:14 AM		
4	283.0	LO ₂ /Kerosene	LO ₂ /LH ₂	Al	Al	11:22 AM		
5	283.0	LO ₂ /Hydrazine	LO ₂ /LH ₂	Al	Al	11:24 AM		
6	283.0	LO ₂ /LH ₂	LO ₂ /LH ₂	Al	Al	11:30 AM		
7	283.0	LO ₂ /LH ₂	LO ₂ /LH ₂	Al	Al	11:33 AM		
8	283.0	LO ₂ /LH ₂	LO ₂ /LH ₂	Al	Al	11:39 AM		
9	283.0	LO ₂ /LH ₂	LO ₂ /LH ₂	Al	Al	11:41 AM		
10	283.0	LO ₂ /LH ₂	LO ₂ /LH ₂	Al	Al	11:46 AM		
11	283.0	LO ₂ /LH ₂	LO ₂ /LH ₂	Ti	Ti	11:50 AM		
12	283.0	LO ₂ /LH ₂	LO ₂ /LH ₂	Al	Al	11:56 AM		
13	283.0	LO ₂ /LH ₂	LO ₂ /LH ₂	Al	Al	11:59 AM		
14	283.0	LO ₂ /LH ₂	LO ₂ /LH ₂	Al	Al	12:04 PM		
15	395.0	LO ₂ /LH ₂	LO ₂ /LH ₂	Al	Al	12:08 PM		
16	395.0	LO ₂ /LH ₂	LO ₂ /LH ₂	Al	Al	12:10 PM		
17	380.0	LO ₂ /LH ₂	LO ₂ /LH ₂	Al	Al	12:16 PM		
18	395.0	LO ₂ /LH ₂	LO ₂ /LH ₂	Al	Al	12:20 PM		
19	395.0	LO ₂ /LH ₂	LO ₂ /LH ₂	Al	Al	12:22 PM		
20	395.0	LO ₂ /LH ₂	LO ₂ /LH ₂	Al	Al	12:25 PM		
21	395.0	LO ₂ /LH ₂	LO ₂ /LH ₂	Al	Al	12:29 PM		
22	377.0	LO ₂ /LH ₂	LO ₂ /LH ₂	Al	Al	12:36 PM		
23	377.0	LO ₂ /LH ₂	LO ₂ /LH ₂	Al	Al	12:38 PM		
24	377.0	LO ₂ /LH ₂	LO ₂ /LH ₂	Al	Al	12:40 PM		
25	394.0	LO ₂ /LH ₂	LO ₂ /LH ₂	Al	Al	12:45 PM		
26	394.0	LO ₂ /LH ₂	LO ₂ /LH ₂	Al	Al	12:49 PM		

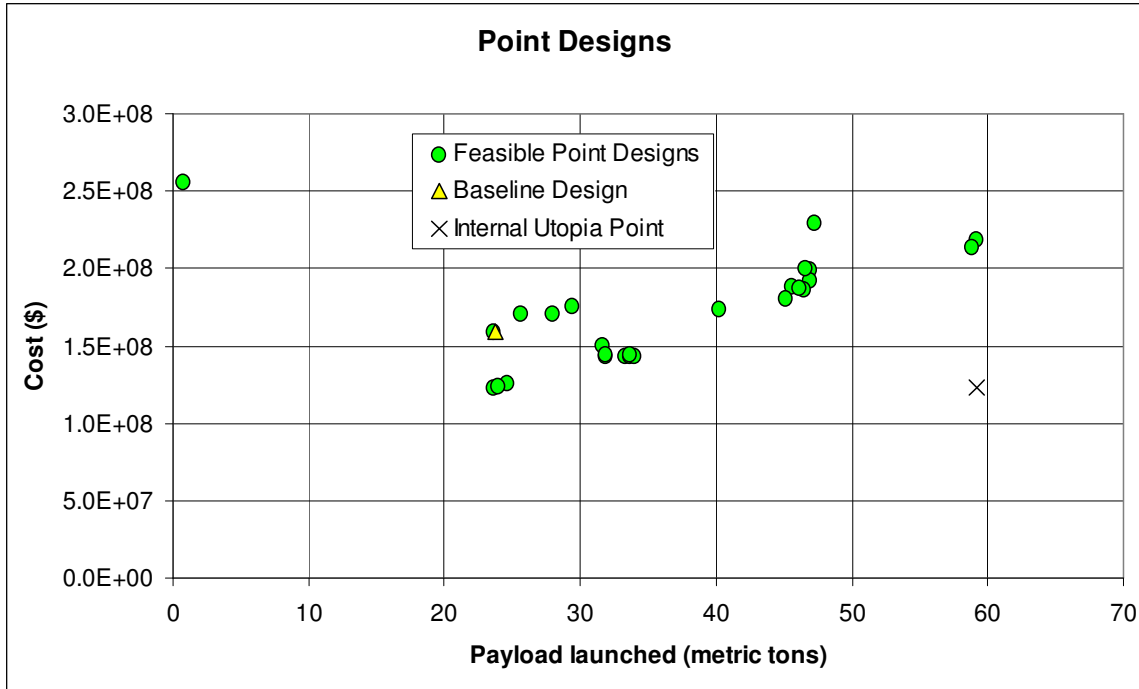


Figure A-6. Optimization group 2 point designs evaluated

A.8 Optimization Group 3

Table A-13. Optimization group 3 composition

Chair	Subsystem	Program/Major
Participant 1	Trajectory	Aeronautics & Astronautics
Participant 2	Propulsion	Aeronautics & Astronautics
Participant 3	Structures	Aeronautics & Astronautics
Moderator	Cost, Systems, Optimizer	Aeronautics & Astronautics

Table A-14. Optimization group 3 feasible design points

Point	m_p (tons)	C (\$)	v_a (Hz)	v_b (Hz)	A_{final} (km)	m_0 (tons)	R_r (m)
1	3.915	2.390E+08	58.3	13.4	662	650.0	4.50
2	3.687	2.350E+08	58.5	13.4	662	650.0	4.50
3	2.845	2.507E+08	59.4	13.9	514	650.0	4.50
4	23.948	1.589E+08	64.1	14.4	413	500.0	4.00

5	34.260	1.499E+08	39.3	3.1	464	823.0	2.30	
6	34.308	1.500E+08	39.3	3.1	464	823.0	2.30	
7	35.392	1.501E+08	39.1	3.1	437	823.0	2.30	
8	34.536	1.456E+08	39.4	3.1	447	823.0	2.30	
9	36.293	1.460E+08	41.9	3.8	411	900.0	2.50	
10	30.479	1.319E+08	51.7	5.8	414	700.0	2.50	
11	16.266	1.055E+08	82.4	14.8	658	400.0	2.50	
12	16.632	8.944E+07	81.4	14.5	504	400.0	2.50	
13	16.213	8.407E+07	81.5	14.5	467	400.0	2.50	
14	19.237	9.154E+07	65.4	9.3	414	550.0	2.50	
15	21.201	9.766E+07	61.1	8.2	410	600.0	2.50	
16	22.543	1.032E+08	59.8	7.8	401	600.0	2.50	
17	7.329	5.448E+07	122.2	32.6	465	200.0	2.50	
18	7.534	5.101E+07	92.4	13.4	458	200.0	1.80	
19	7.569	5.118E+07	69.7	6.4	454	200.0	1.50	
20	9.916	6.070E+07	49.0	3.1	404	300.0	1.50	
21	41.164	1.719E+08	65.7	14.3	403	1000.0	3.80	
22	41.324	1.866E+08	63.6	17.7	401	1000.0	5.00	
23	58.236	2.981E+08	48.4	9.8	496	993.0	4.80	
Point	θ_c (rad)	T_1 (MN)	T_2 (MN)	T_3 (MN)	T_4 (MN)	T_5 (MN)	α_1 (km)	α_2 (km)
1	0.400	15.00	10.00	6.00	3.00	0.00	200.0	300.0
2	0.400	15.00	10.00	6.00	3.00	0.00	200.0	300.0
3	0.400	15.00	10.00	6.00	3.00	0.00	150.0	100.0
4	0.300	10.00	8.00	4.00	1.00	0.00	190.0	100.0
5	0.120	10.40	10.00	10.30	0.40	0.30	17.0	322.0
6	0.120	10.40	10.00	10.30	0.40	0.30	17.0	322.0
7	0.120	10.40	10.00	10.30	0.40	0.30	17.0	300.0
8	0.120	10.00	10.00	10.00	0.40	0.30	17.0	300.0
9	0.120	10.00	10.00	10.00	0.40	0.30	17.0	300.0
10	0.120	9.00	8.00	8.00	0.40	0.30	17.0	300.0
11	0.120	7.00	7.00	7.00	0.40	0.30	17.0	300.0
12	0.120	5.50	5.50	5.50	0.40	0.30	17.0	300.0
13	0.120	5.00	5.00	5.00	0.40	0.30	17.0	300.0
14	0.120	5.50	5.50	5.50	0.40	0.30	17.0	300.0
15	0.120	6.00	6.00	6.00	0.40	0.30	17.0	300.0
16	0.120	6.50	6.00	6.00	0.40	0.30	17.0	355.0
17	0.120	2.50	2.50	2.00	0.40	0.30	17.0	355.0
18	0.120	2.50	2.50	2.00	0.40	0.30	17.0	355.0
19	0.120	2.50	2.50	2.00	0.40	0.30	17.0	355.0

20	0.120	3.00	3.00	2.50	0.40	0.30	17.0	355.0
21	0.120	12.00	11.50	10.00	0.80	0.30	17.0	355.0
22	0.120	12.50	11.50	10.00	0.80	0.30	17.0	355.0
23	0.220	15.00	16.00	19.20	2.70	0.05	2.6	228.0
Point	A _{stage}	Prop. 1	Prop. 2	Rocket Mat	Tank Mat	Time		
1	200.0	LO ₂ /LH ₂	NTO/Hydrazine	Ti	Al	9:51 AM		
2	200.0	LO ₂ /LH ₂	NTO/Hydrazine	Al	Al	9:56 AM		
3	150.0	LO ₂ /LH ₂	NTO/Hydrazine	Al	Al	9:59 AM		
4	200.0	LO ₂ /LH ₂	LO ₂ /LH ₂	Ti	Al	10:13 AM		
5	368.0	LO ₂ /Hydrazine	LO ₂ /LH ₂	Al	Al	10:19 AM		
6	350.0	LO ₂ /Hydrazine	LO ₂ /LH ₂	Al	Al	10:31 AM		
7	350.0	LO ₂ /Hydrazine	LO ₂ /LH ₂	Al	Al	10:35 AM		
8	350.0	LO ₂ /Hydrazine	LO ₂ /LH ₂	Al	Al	10:39 AM		
9	350.0	LO ₂ /Hydrazine	LO ₂ /LH ₂	Al	Al	10:47 AM		
10	350.0	LO ₂ /Hydrazine	LO ₂ /LH ₂	Al	Al	10:55 AM		
11	350.0	LO ₂ /Hydrazine	LO ₂ /LH ₂	Al	Al	11:01 AM		
12	350.0	LO ₂ /Hydrazine	LO ₂ /LH ₂	Al	Al	11:03 AM		
13	350.0	LO ₂ /Hydrazine	LO ₂ /LH ₂	Al	Al	11:05 AM		
14	350.0	LO ₂ /Hydrazine	LO ₂ /LH ₂	Al	Al	11:09 AM		
15	350.0	LO ₂ /Hydrazine	LO ₂ /LH ₂	Al	Al	11:19 AM		
16	350.0	LO ₂ /Hydrazine	LO ₂ /LH ₂	Al	Al	11:28 AM		
17	350.0	LO ₂ /Hydrazine	LO ₂ /LH ₂	Al	Al	11:31 AM		
18	350.0	LO ₂ /Hydrazine	LO ₂ /LH ₂	Al	Al	11:37 AM		
19	350.0	LO ₂ /Hydrazine	LO ₂ /LH ₂	Al	Al	11:39 AM		
20	350.0	LO ₂ /Hydrazine	LO ₂ /LH ₂	Al	Al	11:42 AM		
21	350.0	LO ₂ /Hydrazine	LO ₂ /LH ₂	Al	Al	11:46 AM		
22	350.0	LO ₂ /Hydrazine	LO ₂ /LH ₂	Al	Al	11:50 AM		
23	202.0	LO ₂ /LH ₂	LO ₂ /LH ₂	Ti	Ti	11:54 AM		

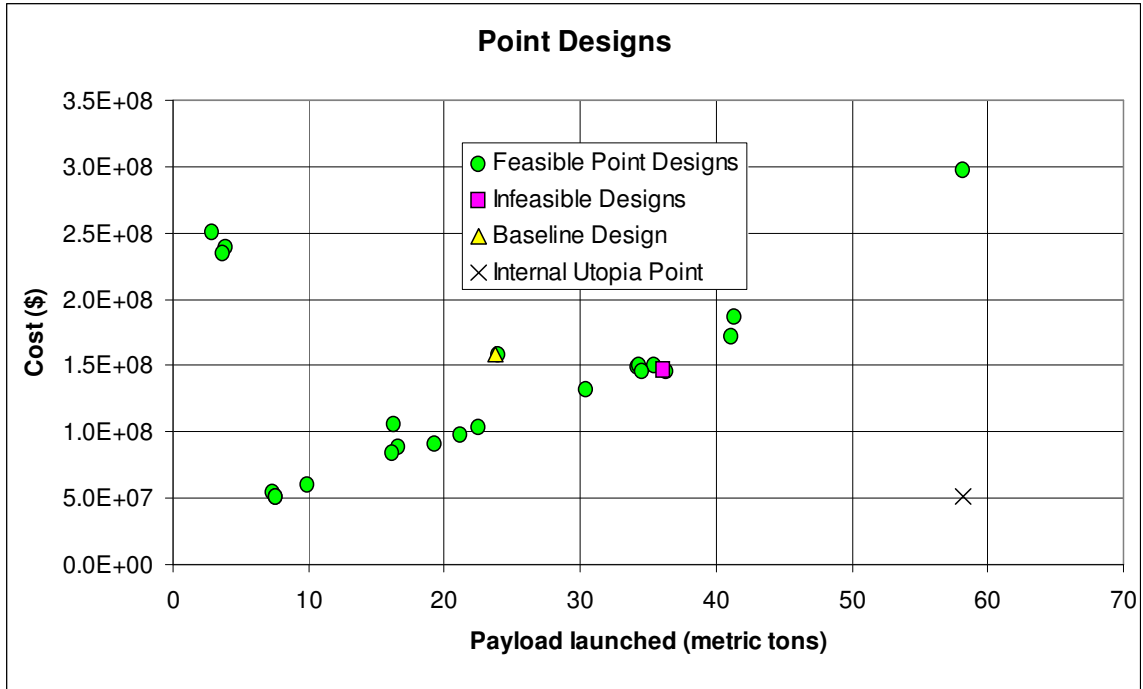


Figure A-7. Optimization group 3 point designs evaluated

References

-
- ¹ Sobieszczanski-Sobieski, J., Agte, J. S., Sandusky, R.R., “Bilevel Integrated System Synthesis (BLISS)”, NASA/TM-1988-208715, August 1998.
- ² Schuman, T., “Integration of System-Level Optimization With Concurrent Engineering Using Parametric Subsystem Modeling,” Master’s Thesis, Aeronautics and Astronautics Dept., Massachusetts Institute of Technology, Cambridge, MA, 2004.
- ³ Miller, G. A., “The Magical Number Seven, Plus or Minus Two: Some Limits on Our Capacity for Processing Information,” *The Psychological Review*, Vol. 63, 1956, pp. 81-97.
- ⁴ Parkin, K., Sercel, J., Liu, M., and Thunnissen, D., "ICEMaker: An Excel-Based Environment for Collaborative Design," 2003 IEEE Aerospace Conference Proceedings, Big Sky, Montana, March 2003.
- ⁵ Cohanin, B. E., Hewitt, J. N., de Weck, O., “The Design of Radio Telescope Array Configurations using Multiobjective Optimization: Imaging Performance versus Cable Length,” *The Astrophysical Journal Supplement Series*, Vol. 154, October 2004, pp. 705-719.
- ⁶ Bairstow B. K., de Weck O.L., Sobieszczanski-Sobieski J., “Multiobjective Optimization of Two-Stage Rockets for Earth-To-Orbit Launch”, AIAA-2006-1720, 2nd AIAA MDO Specialist Conference, Newport, RI, May 1-4, 2006
- ⁷ Braun, R. D., Powell, R. W., Lepsch, R. A., Stanley, D. O., and Kroo, I. M., “Comparison of Two Multidisciplinary Optimization Strategies for Launch Vehicle Design,” *Journal of Spacecraft and Rockets*, Vol. 32, No.3, May-June 1995, pp. 404-410.
- ⁸ Schoonover, P. L., Crossley, W. A., and Heister, S. D., “Application of a Genetic Algorithm to the Optimization of Hybrid Rockets,” *Journal of Spacecraft and Rockets*, Vol. 37, No.5, September-October 2000, pp. 622-629.
- ⁹ Tsuchiya, T., and Mori, T., “Optimal Conceptual Design of Two-Stage Reusable Rocket Vehicles Including Trajectory Optimization,” *Journal of Spacecraft and Rockets*, Vol. 41, No.5, September-October 2004, pp. 770-778.
- ¹⁰ Taylor, C., “Single Stage to Orbit Rocket Model,” Massachusetts Institute of Technology, Cambridge, MA, 2005.
- ¹¹ Sobieszczanski-Sobieski, J., “External Fuel Tank Model,” AIAA Short Course on Multidisciplinary Design Optimization, NASA Langley Research Center, Hampton, VA, 2002.

-
- ¹² Kauffmann, J. W., Sippel, M., Schmid, V., “Mission Adapted Preliminary Design of Solid Rockets for Space Launch Systems,” *Joint Propulsion Conference and Exhibit*, AIAA, Reston, VA, 1999.
- ¹³ Tobias, M., Sauvageau, D. R., Hines, M., Geiser, N. L., “Five-Segment Booster Abort to Orbit Studies,” *Joint Propulsion Conference*, AIAA, Reston, VA, 2002.
- ¹⁴ *U.S. Standard Atmosphere, 1962*, U.S. Government Printing Office, Washington, D.C., 1962.
- ¹⁵ Isakowitz, S. J., Hopkins, J. B., and Hopkins, J. P., Jr., *International Reference Guide to Space Launch Systems*, 4th ed., AIAA, Virginia, 2004, pp. 109-146.
- ¹⁶ Ahuja, R. K., Orlin, J. B., Tiwari, A., “A Greedy Genetic Algorithm for the Quadratic Assignment Problem,” *Computers and Operations Research*, Vol. 27, 2000, pp. 917-934.
- ¹⁷ Ross, S. M., *Introduction to Probability and Statistics for Engineers and Scientists*, 2nd ed., Academic Press, San Diego, CA, 2000, pp. 291-299.